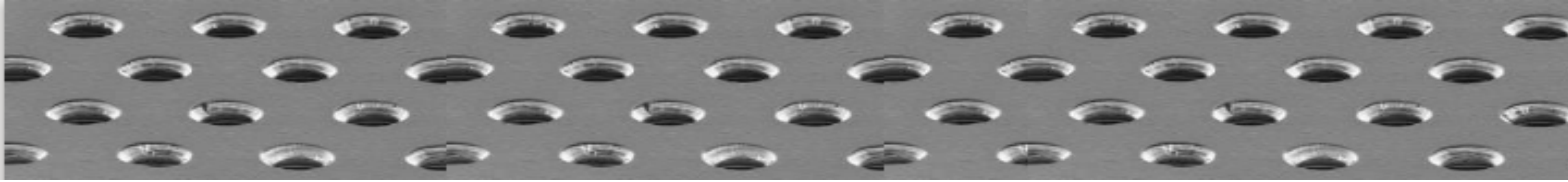

A seminar on

Searches for exotic Higgs boson decays and the CMS muon spectrometer upgrade

By

Aashaq Shah

Work from my PhD thesis: CERN-THESIS-2020-202

Queen Mary University of London

Particle Physics Research Center (PPRC)
Queen Mary University of London, UK

Part I: CMS muon upgrade

The LHC

The Large Hadron Collider (LHC) at CERN is located in a circular tunnel 27 km in circumference. The tunnel is buried around 100 m underground

It straddles the Swiss and French borders on the outskirts of Geneva

The proton beams are accelerated with the speed nearly equal to the speed of light and collided mainly at four points

The collision points are the hearts of the main experiments, known by their Acronyms: ALICE, ATLAS, CMS, and LHCb

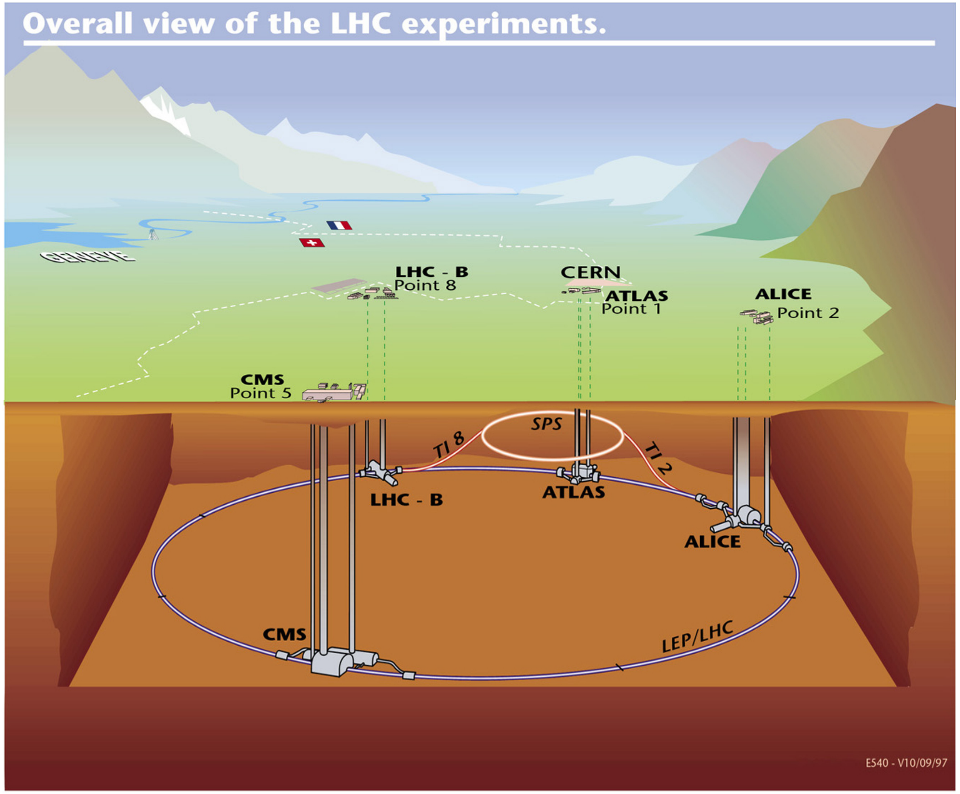

Compact Muon Solenoid (CMS)?

TDR CERN-LHCC-*2017*-012

The CMS Experiment

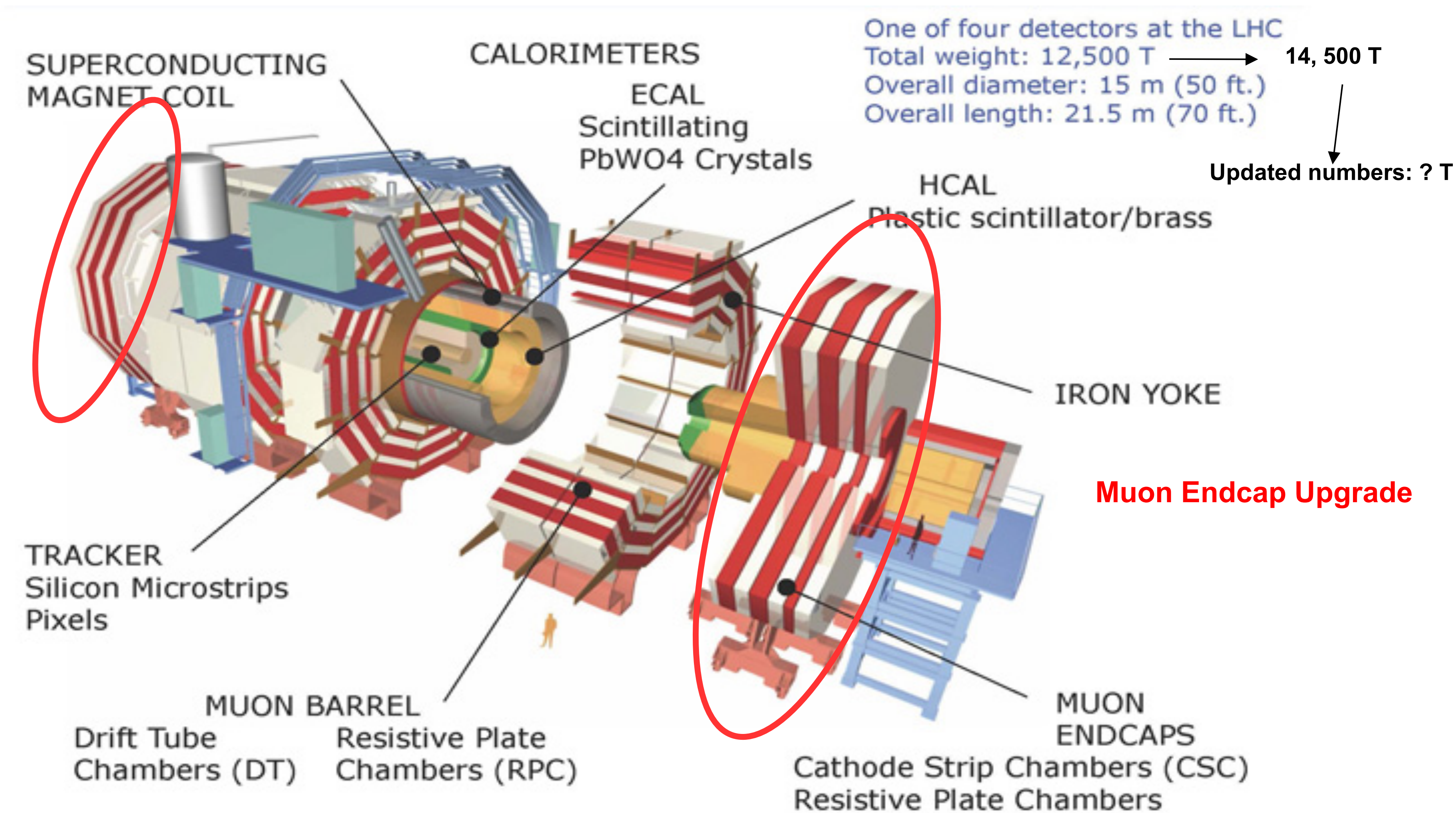

TDR CERN-LHCC-*2017*-012

The CMS Muon Endcap Upgrade (1/1)

- **LHC is going for the major upgrade**

- **Why Upgrade?**
  - To increase its discovery potential by extending the search sensitivity
  - Search for new physics that may validate/invalidate BSM theories like 2HDM, etc.
  - Access rare decays e.g., $h \rightarrow 4\mu$, B-meson decay $B \rightarrow 2\mu$

- **Two major aspects of the upgrade resulting the HL-LHC:**
  - The increase of the center-of-mass energy to 14 TeV in order to provide more energy during the collisions and reveal massive particles
  - Gradual increase of the luminosity up to 5-7 × 10^{34} $cm^{-2}s^{-1}$ (resulting HL-LHC) to access very rare physics phenomena

- **The HL-LHC**
  - ❑ Experiments to face high rates
  - ❑ Problems CMS muon system would face

    Increase of the background rate in the forward region |η| > 1.6 provoking a rise of the level-1 muon trigger rate

    High-radiation background will accelerate the aging of the current CSC system resulting the loss of performance in the high eta region endocarp region

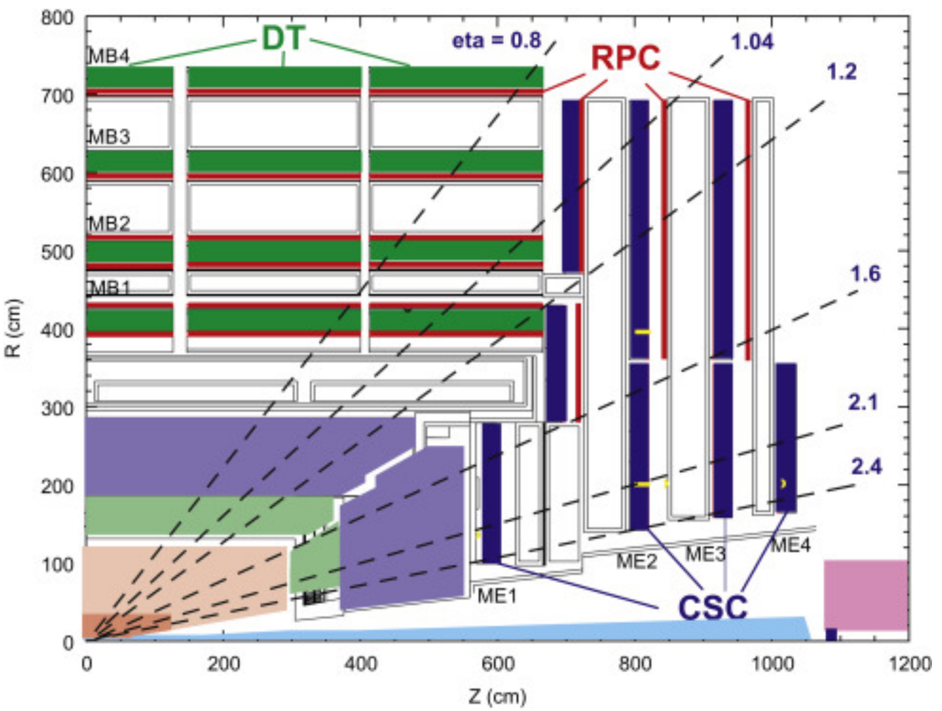

The CMS Muon Endcap Upgrade (1/2)

- Muon upgrade of the CMS required in order to maintain its high level of performance particularly in the region with |η| > 1.6

- **Muon detector requirements**
  - Detector should be able to cope up with high rate
  - Good position resolution and temporal resolution
  - Should be radiation resistant

- Solution proposed by the CMS Collaboration which consisting of introducing an additional gaseous detectors known as GE1/1

- **Technology based on Gas Electron Multiplier (GEM)**
  - Provide fast triggering
  - Precise tacking
  - Will help to improve muon trigger
  - Can sustain the high radiation environment for longer term

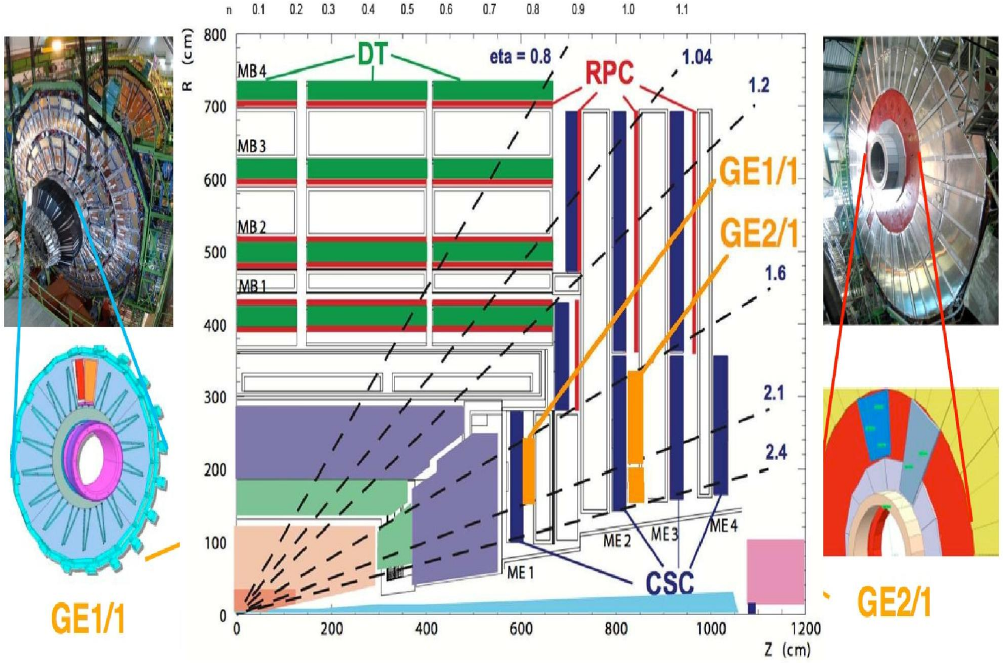

Gas Electron Multiplier (GEM)

- Concept of GEM introduced by Fabio Sauli*

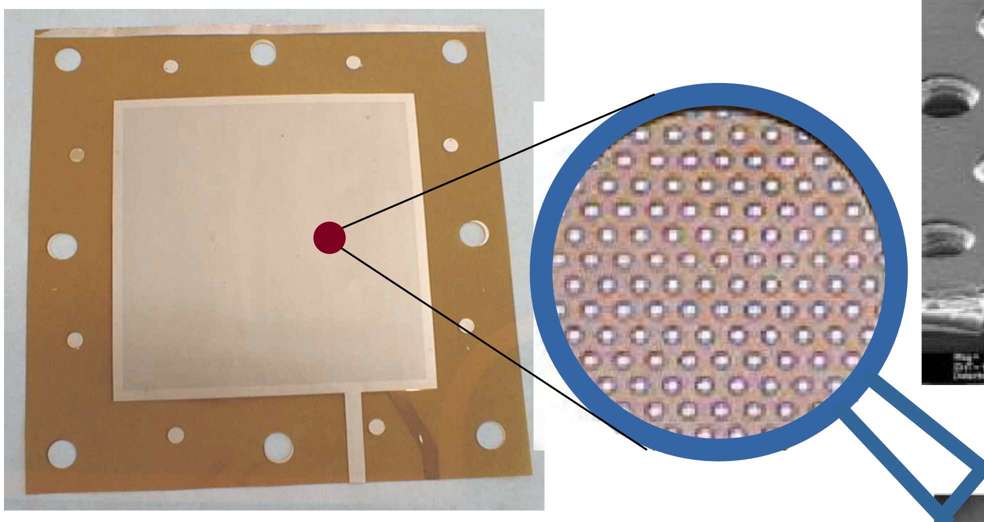

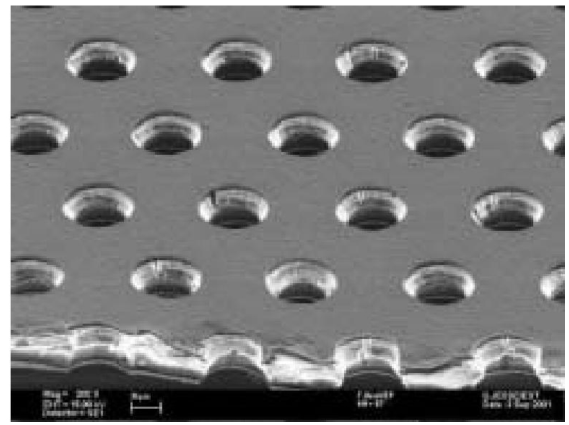

Electron Microscope view of a GEM

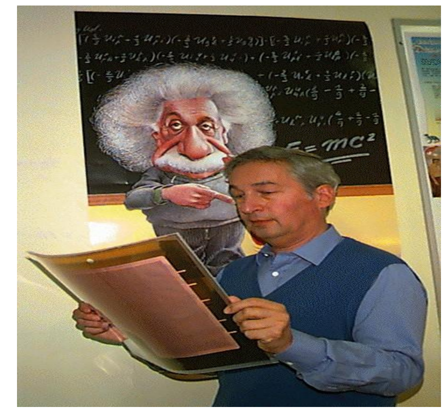

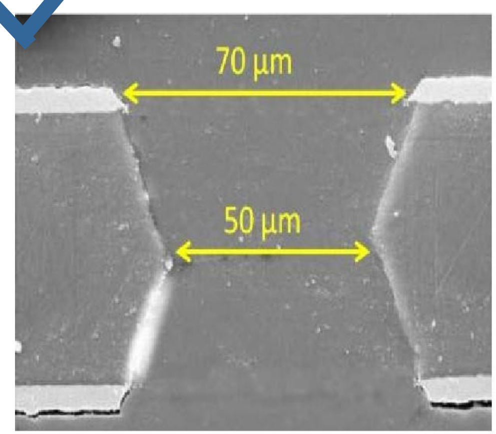

$$D = 70\ \mu\mathrm{m}$$
$$d = 50\ \mu\mathrm{m}$$
$$p = 140\ \mu\mathrm{m}$$

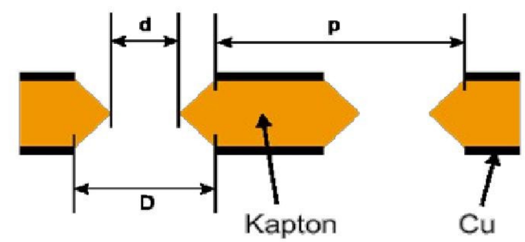

- Thin double-sided metal-coated polymer pierced by a high density of holes

- Typical parameters
  - **Kapton metal coated~ 50µm**
  - **Pitch~140µm**
  - **Cu thickness~5µm**
  - **Hole density ~50 to 100mm^{-2}**

*F. Sauli, Nucl. Inst. Meth. A386 (1997) 531-5341

Working Principle

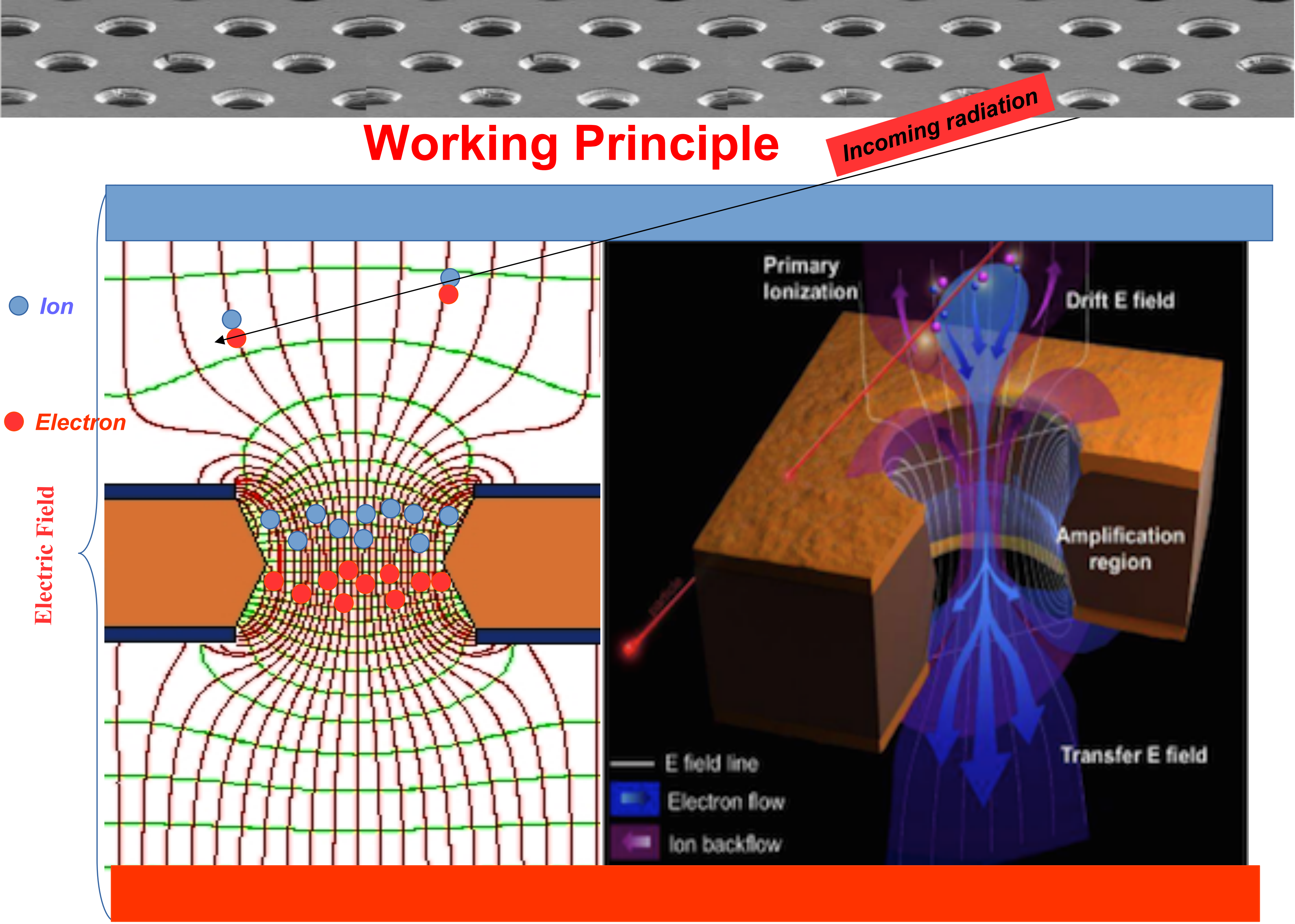

- Ionisation Process, why are GEM's then fast?

Tripple GEM

- Working: amplification takes place in holes
- Ar and CO_2 (70:30)% baseline gas mixture
- Single stage amplification not enough
- An arrangement of three cascaded GEM foils sandwiched between readout and drift boards commonly known as a ”triple-GEM detector”
- Gap Config. (3/1/2/1) mm to ensure the best timing resolution
- **Fields**
  - Drift field ~2.5 kV/cm
  - Induction field ~ 5kV/cm
  - Transfer fields ~ 3kV/cm
  - Across hole ~80-100kV/cm
- Structure allows high charge amplification factor (up to several 10^5) for modest high voltage without electrical breakdown

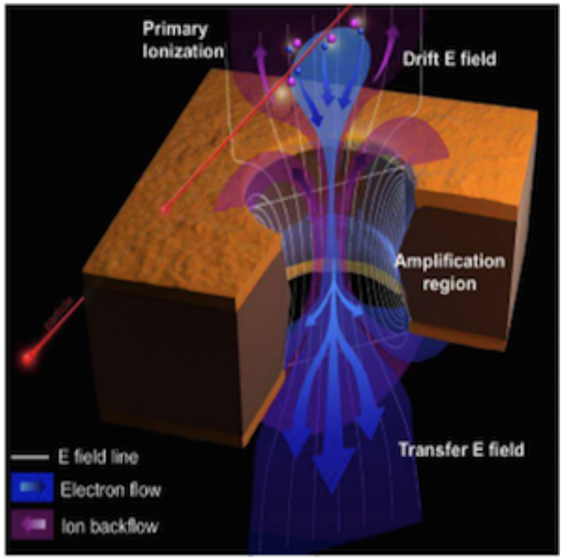

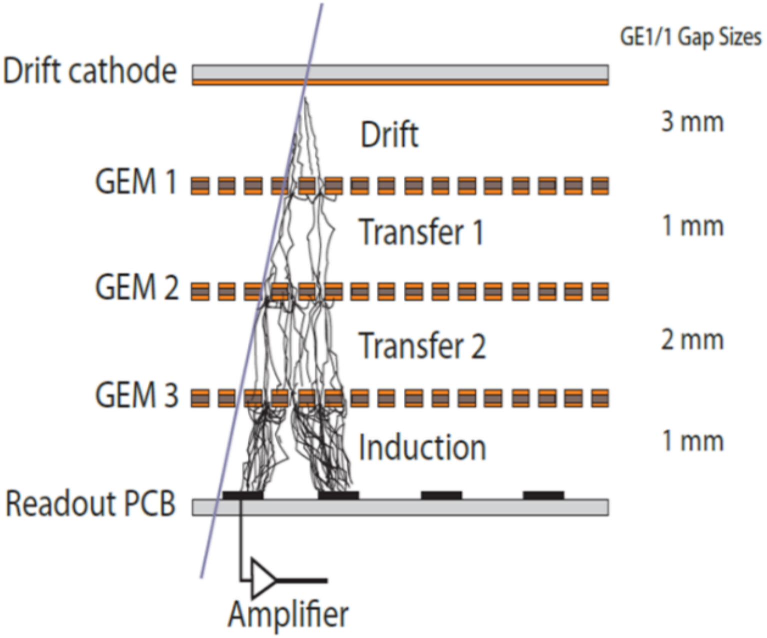

The CMS Muon Endcap Upgrade using GEM technology

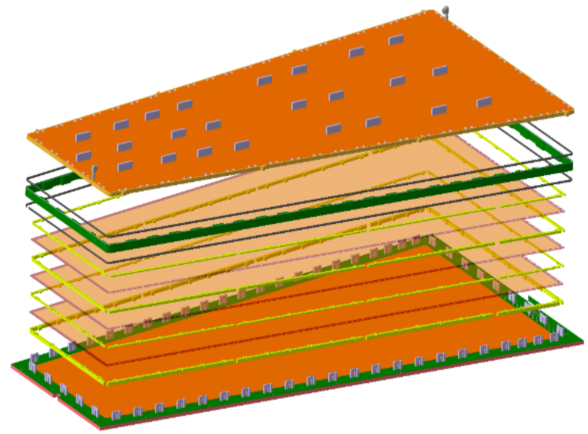

- New chambers will be based on the GEM technology, which can operate at very high rates with good performance
- After several years of R&D program, many versions of GE1/1 chambers have been built so far by improving their design in each release

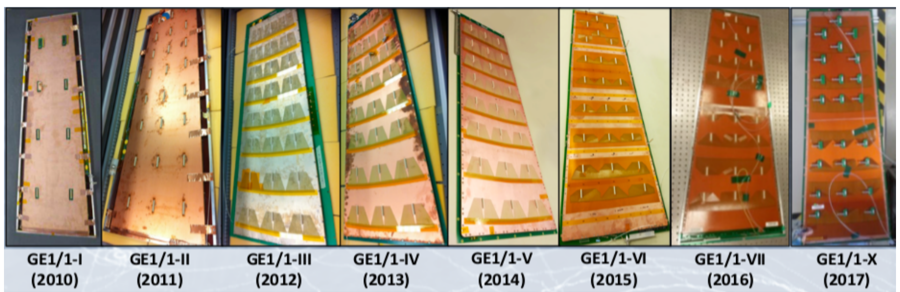

Evolution of GE1/1 detector's since 2010 from generation-I to X (2017)

Mechanical Stretching

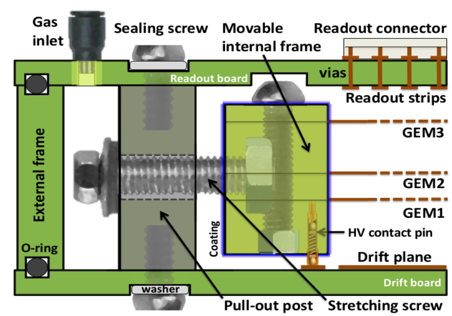

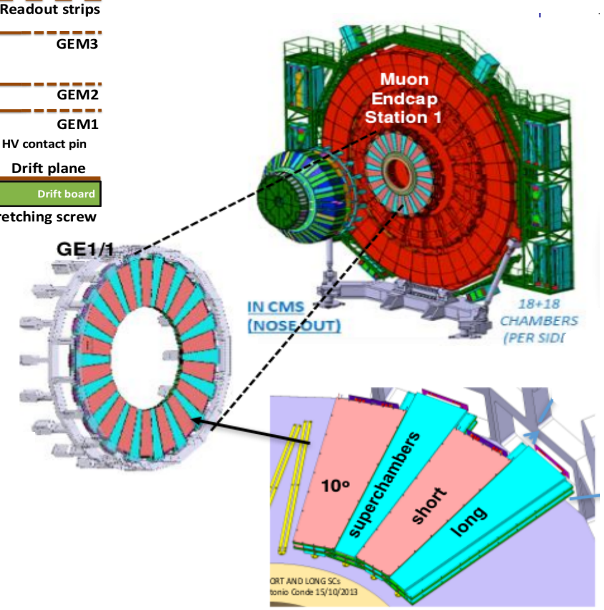

- Mechanical constraints in the GE1/1 station, allow the use of two versions of chambers to have maximum detection coverage, the long GE1/1-L witha length of 128.5 cm and the short GE1/1-S of 113.5 cm

Installation in LS2

Nuclear Inst. and Methods in Physics Research, A 918 (2019) 67–75

Contents lists available at ScienceDirect

Nuclear Inst. and Methods in Physics Research, A

journal homepage: www.elsevier.com/locate/nima

ELSEVIER

Layout and assembly technique of the GEM chambers for the upgrade of the CMS first muon endcap station

Aashaq Shah (corresponding author)

Gain Measurements

- The gain of GE1/1-IV chamber is estimated for gas mixtures
  - Ar/CO_2 (70/30)
  - Ar/CO_2 /CF_4 (45/15/40)
- It is observed that the gain for GE1/1-IV is higher in Ar/CO_2
- Compared to $Ar/CO_2/CF_4$, and is due to electron absorption by CF_4 quencher
- The gain measurements are also performed on GE1/1-IV and GE1/1-VI detectors
- The results show that the gain is higher for sixth generation GE1/1-VI compared to the fourth generation GE1/1-IV
  - Attributed to GEM foil orientation
  - GE1/1 use single mask foils with asymmetrical holes
  - Holes facing incident radiation on narrow side show higher
  - Gain compared to wide side holes

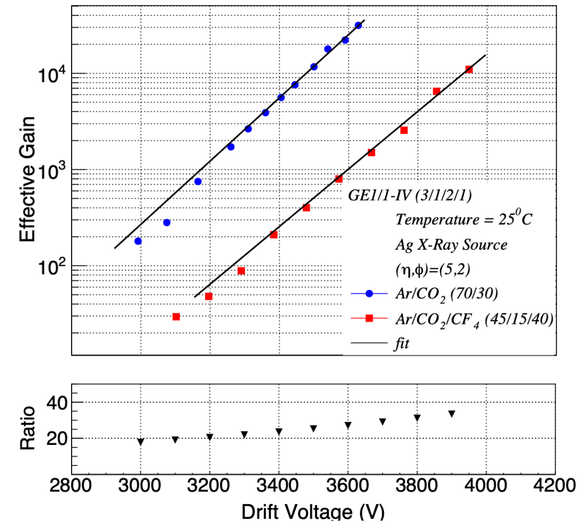

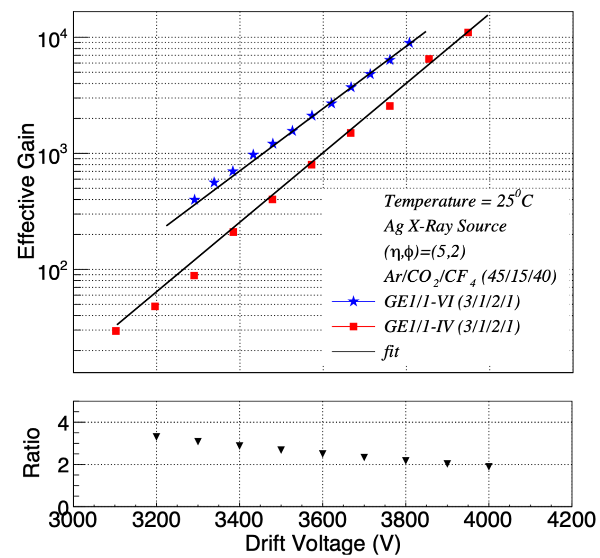

Double-mask GEM hole

Single-mask GEM hole

Beam tests: Efficiency and timing

- CERN's Super Proton Synchrotron (SPS) has been used
- Tracking telescope used as developed by RD51 Collaboration
  - Consists of three scintillators S1, S2 and S3, three 10 cm × 10 cm GEM detectors
  - Movable structure allowing translations in φ and η directions to allow the beam alignment with different GE1/1 readout sectors

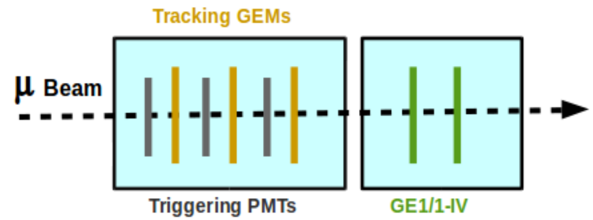

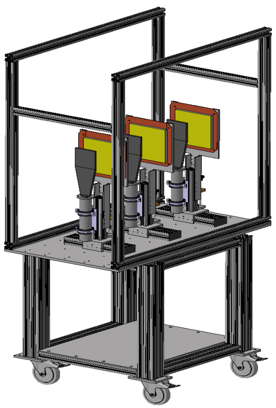

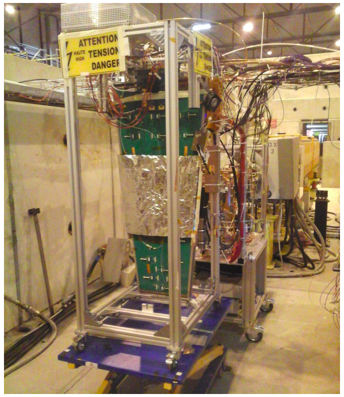

- **98% efficiency is estimated at a gain of 2 x 10^4**
- **Timing resolution ~6ns an essential parameter to ensures that detector can act as a fast triggering system in CMS and hence can identify correct bunch crossing**

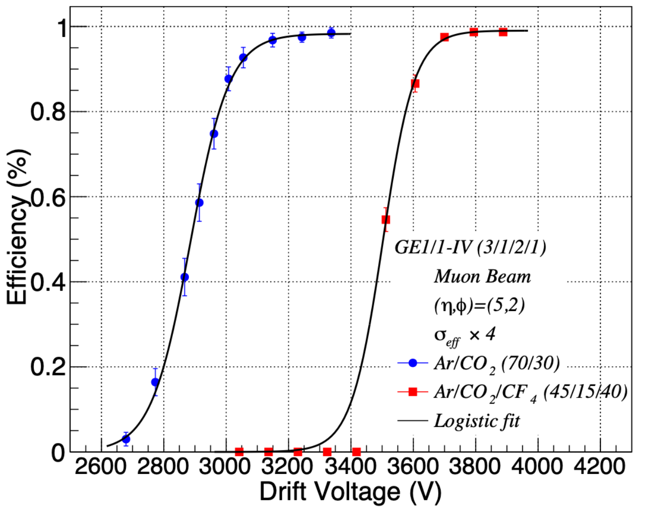

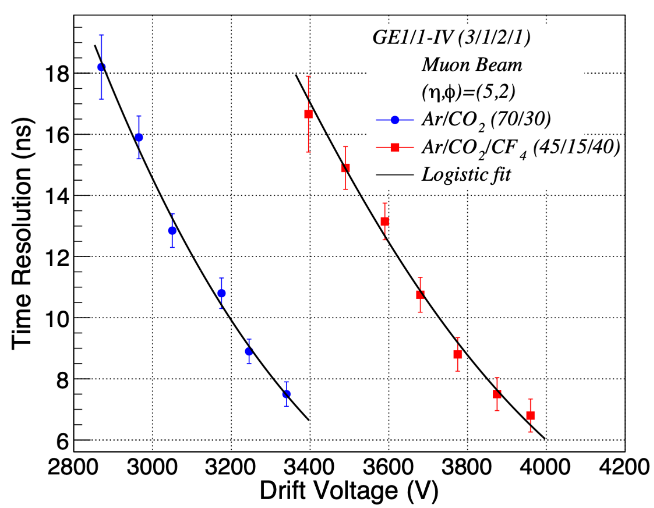

Timing and Rate Capability

Timing measurements

- Results of timing resolution expressed as a function of gain by fitting timing data for Ar/CO_2 and $Ar/CO_2/CF_4$
- An improvement of ~24% by adding CF_4 component in Ar/CO_2

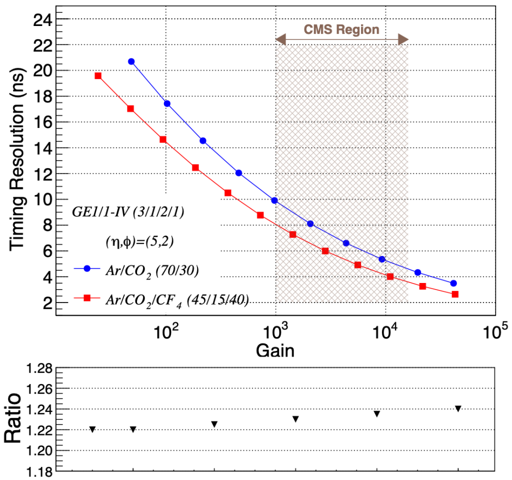

Rate Capability

- The problem with traditional detectors such as RPCs is the limited response at high interaction fluxes
- At several Hz/mm^2 , the space-charge density evokes a local perturbation of the electric field leading a drop in gain
- Maximum expected flux in the CMS endcaps is nearly 100 Hz/mm^2 (10 kHz/cm^2), the chambers should tolerate such high particle rates without any loss in performance
- Rate capability of GE1/1 chambers is measured and it is found that the effective gain remains stable up to 10^5 kHz/cm^2
- Demonstrated that GEM's can be used very well in the CMS

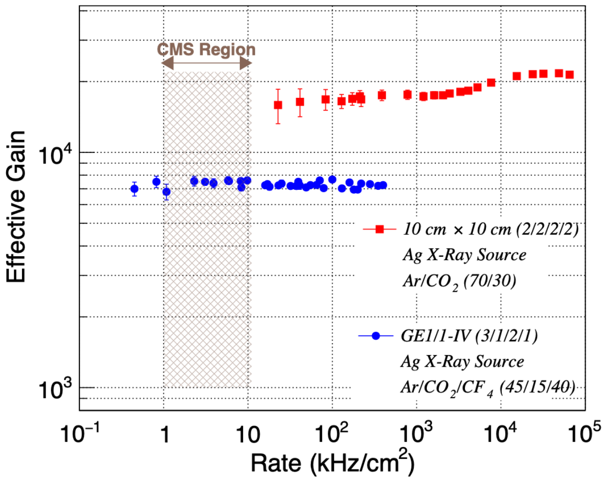

Discharge Probability

- In case of intense particle fluxes, operating a detector at high gains ($\sim 10^4$) increases the probability of producing discharges which could damage the detector
- Discharges initiate when the charge exceeds Raether limit

- Gain is set to extremely high value ranging from 4 to 6 $\times 10^5$ and the detector is irradiated by densely ionizing a-particles from ^{241}Am source
- The actual discharge probability is calculated by extrapolation to CMS region
- Alpha particle from the ^{241}Am produces nearly hundred times more primaries than a MIP, the discharge probability is divided by this factor and is observed to be less than 10^{-11} for MIPs in standard CMS operating conditions

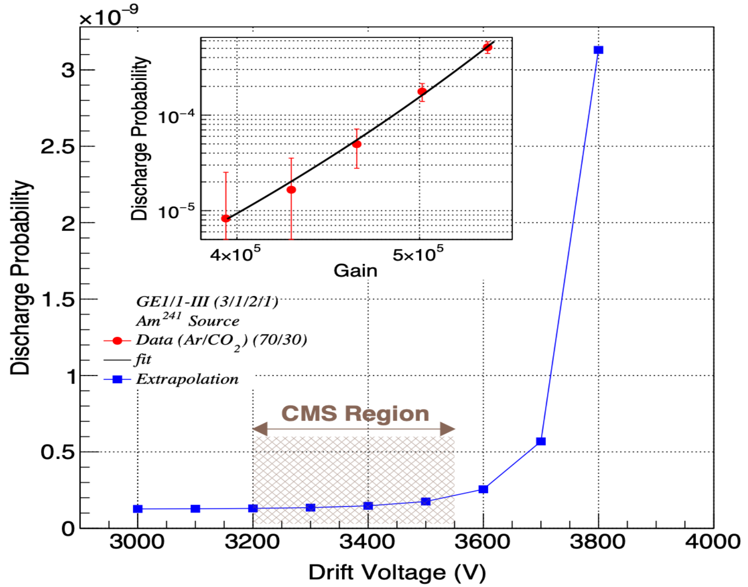

Performance

- **Master plot of GE1/1 detectors for Ar/CO_2 showing**
  - **Gain**
  - **Discharge probability**
  - **Efficiency**
  - **Timing resolution**
- **Similar plot has been obtained for Ar/CO_2/CF_4**
- **The shaded region corresponds the operation regime of the GE1/1 detectors in the CMS**

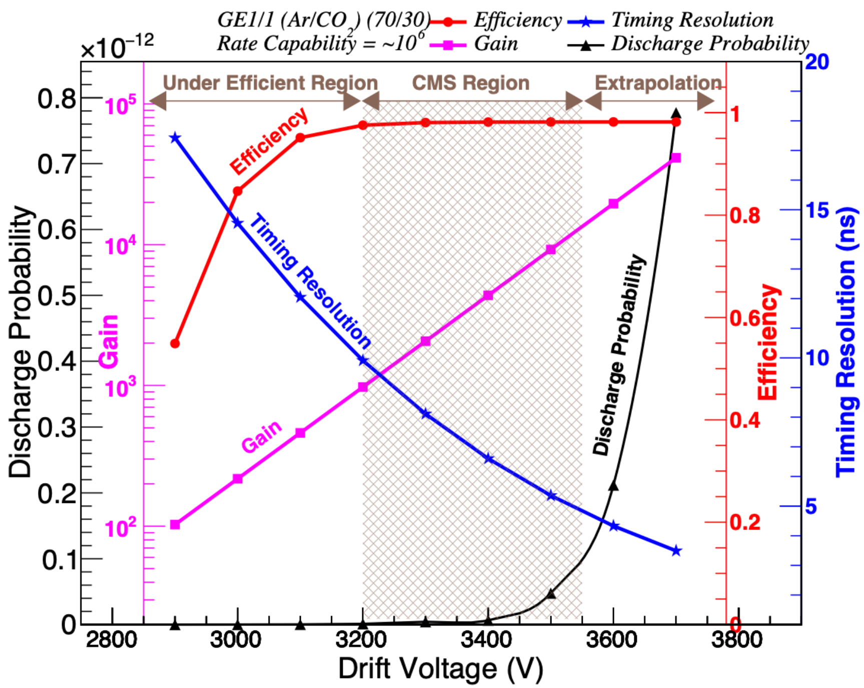

Nuclear Inst. and Methods in Physics Research, A 972 (2020) 164104

Contents lists available at ScienceDirect

Nuclear Inst. and Methods in Physics Research, A

journal homepage: www.elsevier.com/locate/nima

ELSEVIER

Performance of prototype GE1/1 chambers for the CMS muon spectrometer upgrade

Aashaq Shah (corresponding author)

Current status of CMS GE1/1 project

- The CMS Collaboration proposed the use of GEM in the muon endcap in 2009
- After, several years of R&D, various generations of GE1/1 chambers were produced with generation-X in 2017 as the latest and final
- Ten such chambers have been installed inside the CMS experiment during 2017 EYETS and are providing full operational experience
- All the 144 GE1/1 chambers have been produced and validated (Dec. 2018) and will be installed in CMS experiment during LS2 (2019-2020)
- All the chambers integrated with the CMS and commissioning almost complete

A photograph taken in December 2018 showing some of the large size GE1/1 chambers that have been constructed and stored in racks at CERN Prevessin building 904.

A huge success!

Part II: R&D on GEM foils

- **GE1/1 detectors requires large area foils**
- **Double-mask foil technology limited up to 40 cm X 40 cm**
- **Single-mask technology are used in GE1/1**
- **Single mask production techniques results asymmetrical holes**
  - **Important to characterize these foils for GE1/1 upgrade**

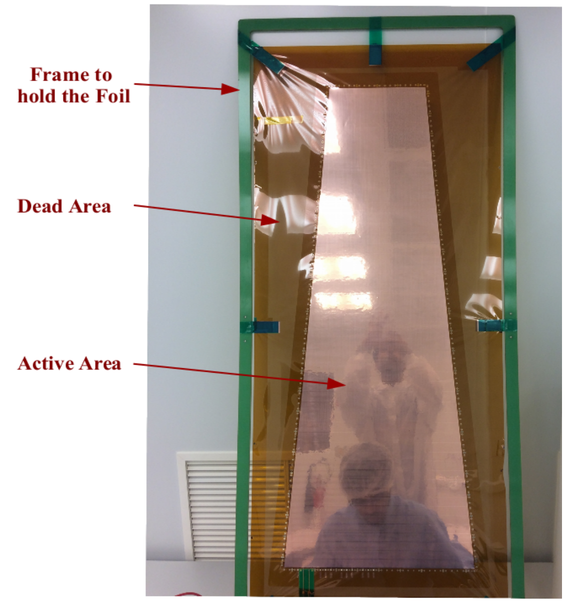

SEM: Double-mask

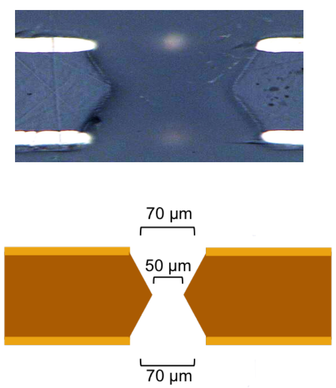

SEM: Single-mask

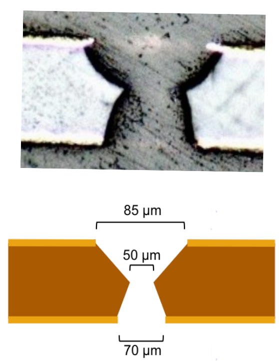

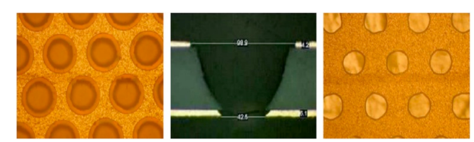

Question:* *Is there any effect on the detector properties due to this hole Asymmetry?

Is it important for GE1/1 Chambers?

GEM Detector (3/2/2/2) mm

- How to find an answer?

GEM Gap Config. (General 3/2/2/2) mm or (CMS gap 3/1/2/1) mm

Single-Mask:
Asymmetric Single Hole Structure

Source direction 1

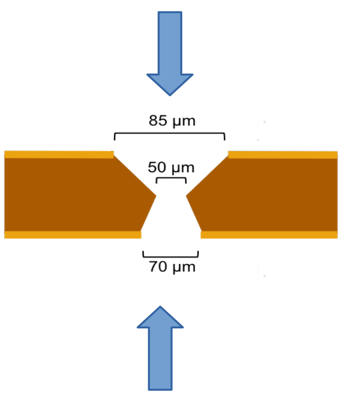

Source direction 2

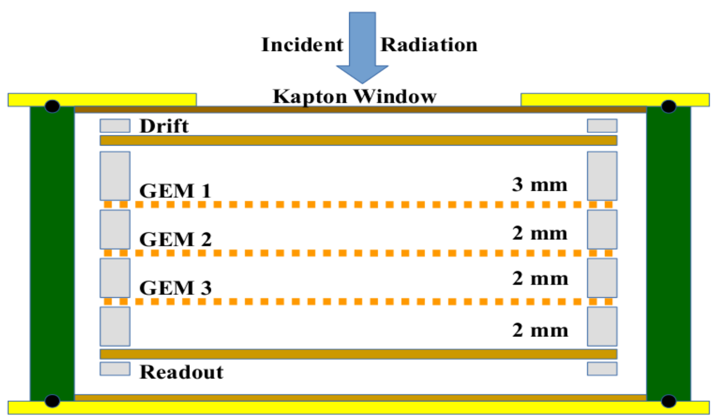

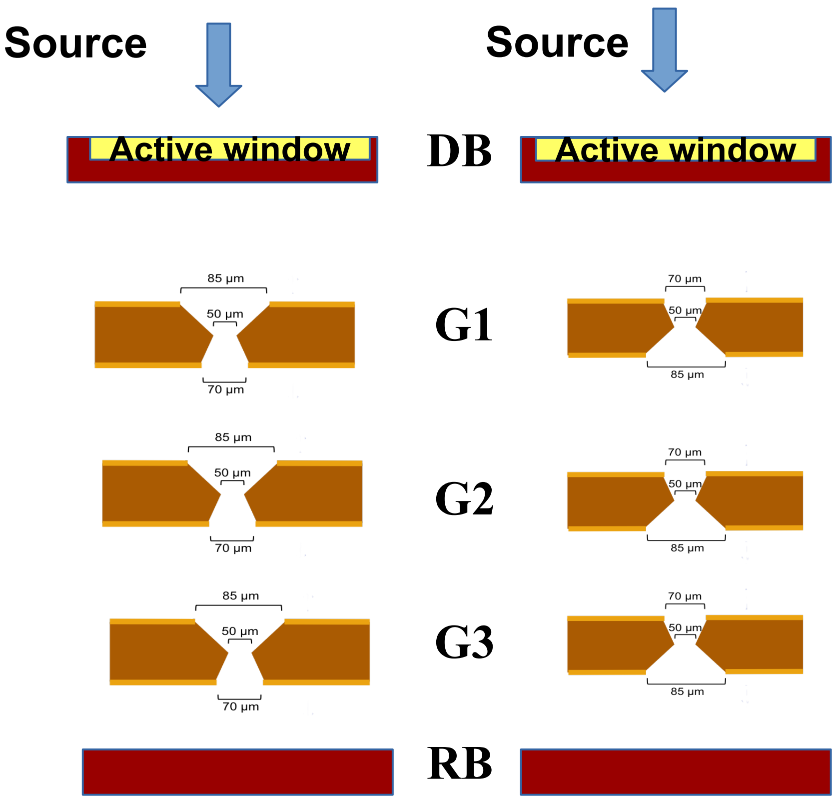

- **Perform testing with one particular orientation**
- **Open the detector and change the orientation of the foils and perform the testing again**

- **Problem: Error prone as opening and closing may introduce other effects, like dust, gap variation etc**

Symmetric Detector (2/2/2/2)mm

- **To Answer:** **Realized a detector with symmetric 2/2/2/2 mm Gap. Conf.**
- **The detector could be irradiated both the ways without opening it**

Symmetric Gap Config. 2/2/2/2

Single-Mask:
Asymmetric Single Hole Structure

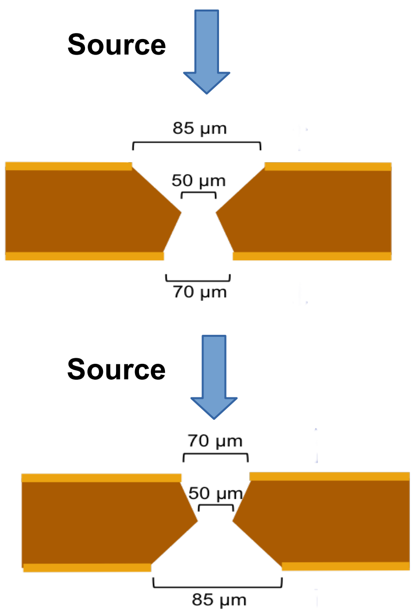

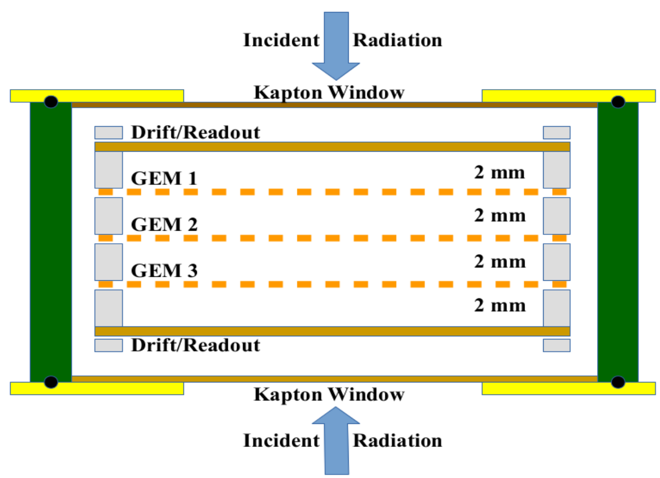

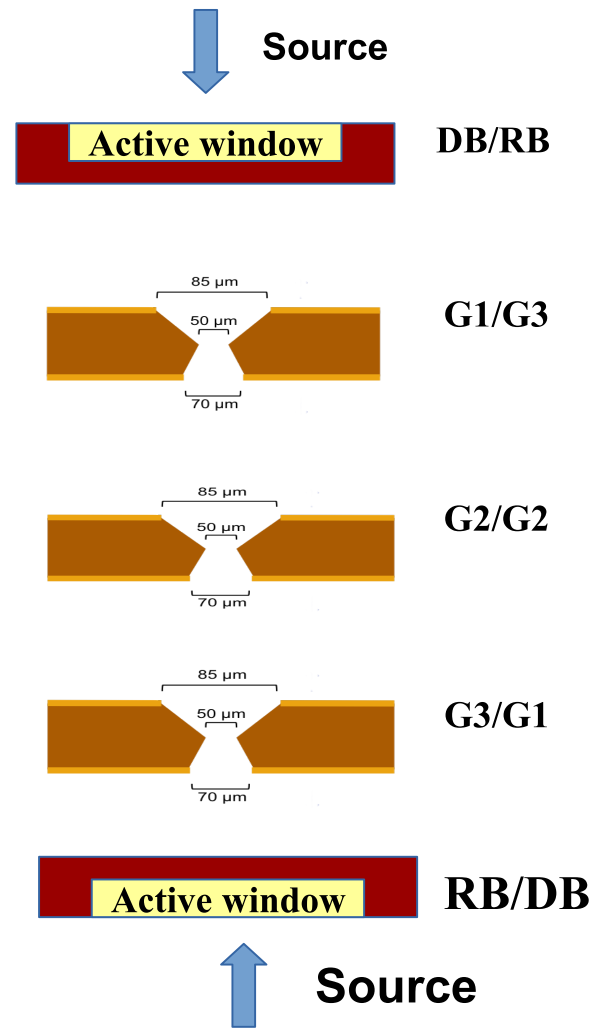

- **Advantage:** No need to open the detector for foil inversion and hence less error prone

Gain Measurements

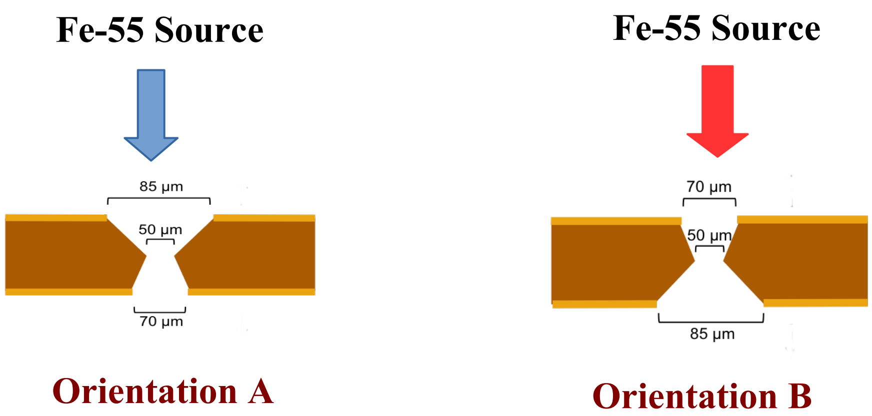

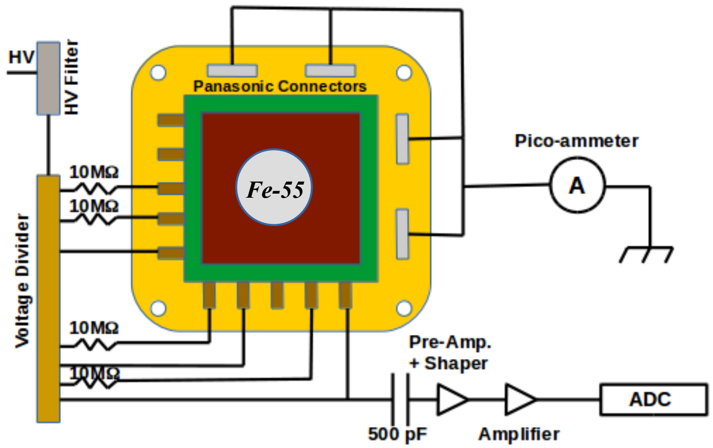

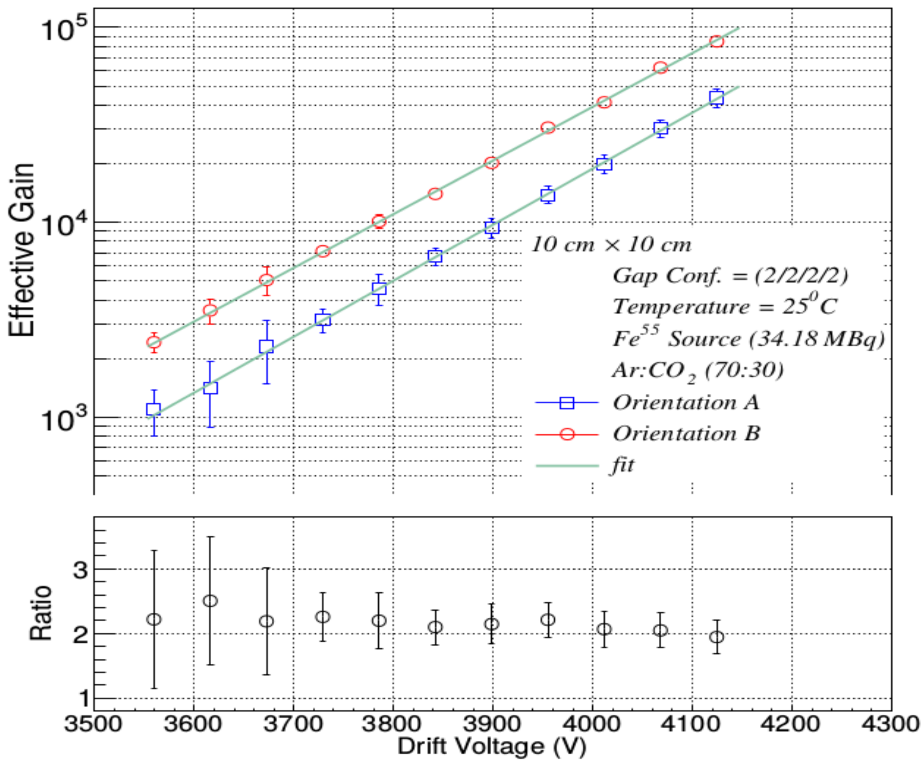

Detector irradiated on both the directions using Fe-55 source

- The gain is observed to be two times higher when Orientation B is facing the source compared to Orientation A
- The best value of energy resolution of around ~23.71%±0.02 has been measured for Orientation A at a gain of 2.2 x10^4
- For Orientation B, ~18.06% ±0.01 has been obtained at a gain of 2.2 x10^4

Charging-up behavior

- The durability of the detector's gain over time is essential for reaching a stable performance of gas detectors, manifested in energy resolution and detector efficiency.

- Variations in the detector gain over the first hours of operation have been perceived in gaseous detectors, such as in GEMs, incorporating insulating electrode substrates.

- The gain variation has been connected to charging-up of the detector's insulating surfaces (Kapton) that modifies the electric field in the charge-multiplication region

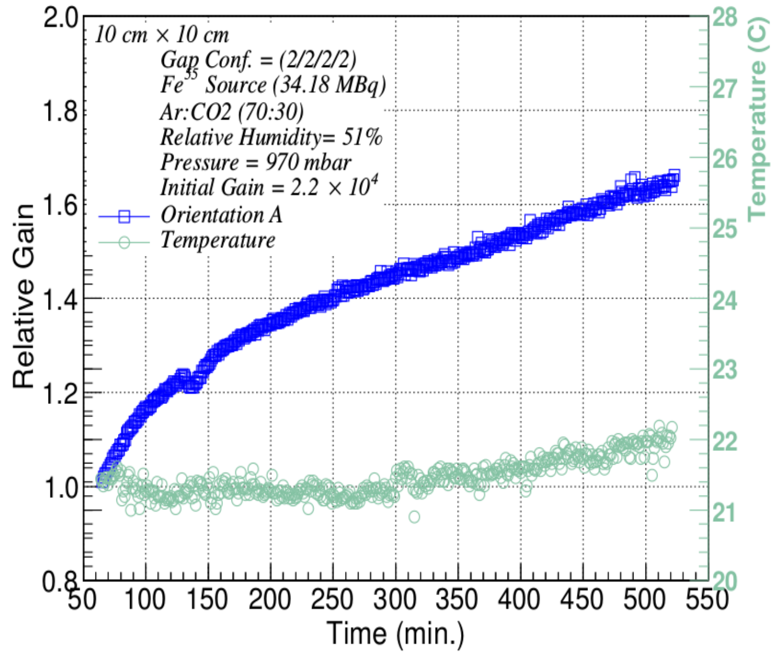

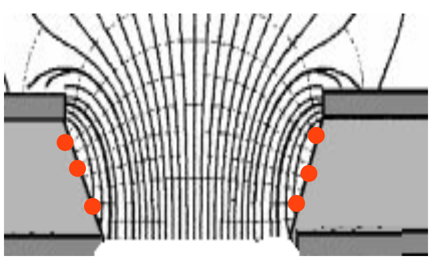

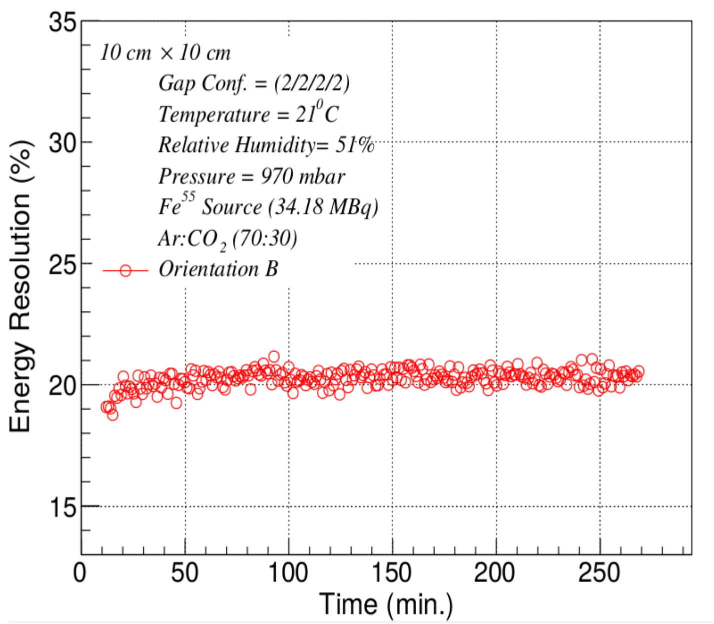

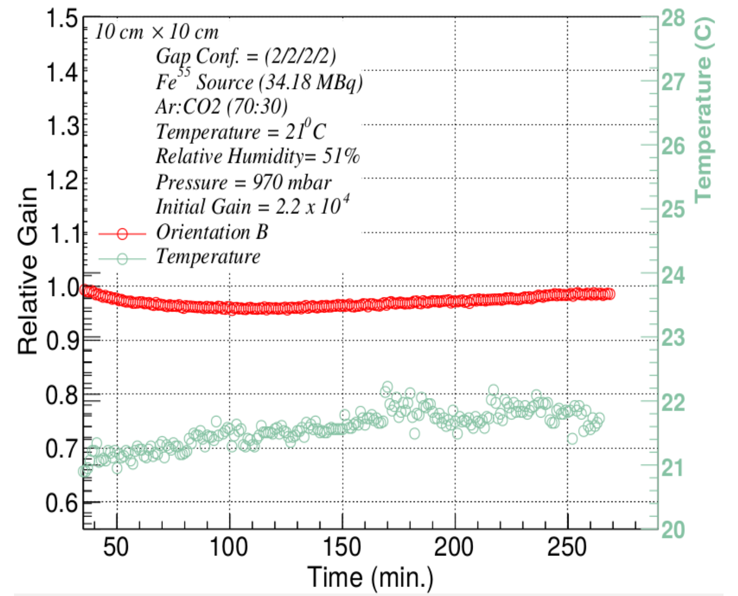

Gain Uniformity Measurements

- **Fluctuations in Gain could be attributed to**
  - **The gas composition**
  - **Local contamination**
  - **Non-uniformity of the hole geometry**
  - **Poor stretching, etc**

- **Active window (10 cm X 10 cm) divided into 7 X 7 = 49 sectors with each Sector approximately 1 cm x 1 cm and each sector irradiated with Fe-55**

- **Gain of each sector was measured and normalized to 2 x 10^4**
  - **Gain fluctuations ~10-15%**

- **Energy resolution of each sector was measured**
  - **The energy resolution over the active area varies from 18% to 22% in ‘Orientation A’ and 24% to 28% in ‘Orientation B’.**

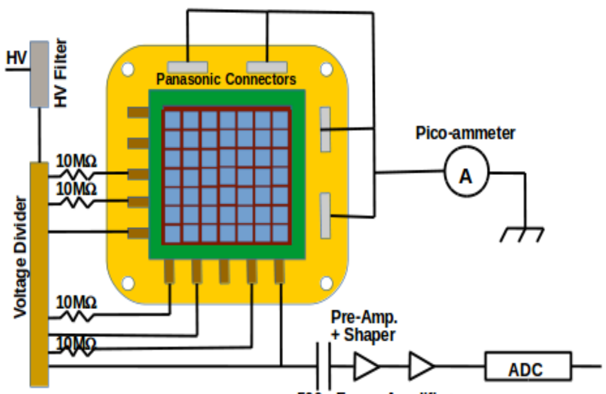

Actual detector

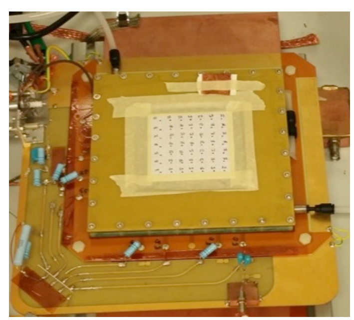

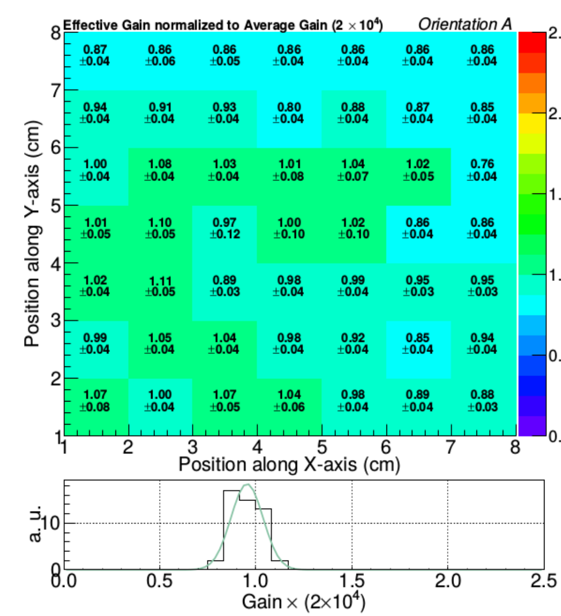

Nuclear Inst. and Methods in Physics Research, A 936 (2019) 459–461

Contents lists available at ScienceDirect

ELSEVIER

Nuclear Inst. and Methods in Physics Research, A

journal homepage: www.elsevier.com/locate/nima

Impact of single-mask hole asymmetry on the properties of GEM detectors

Aashaq Shah [a,*], Archana Sharma [b], Ashok Kumar [a], Jeremie Merlin [b], Md. Naimuddin [b],

Aashaq Shah (leading and corresponding author)

Development first Indian GEM foil

- GEM foils have attracted significant interest from the nuclear and particle physics communities, as they are excellent candidates to be used in tracking detectors
- Micropack signed a TOT agreement with CERN for the development of GEM foils in India and has been successful in realizing 10 cm × 10 cm double mask GEM foils

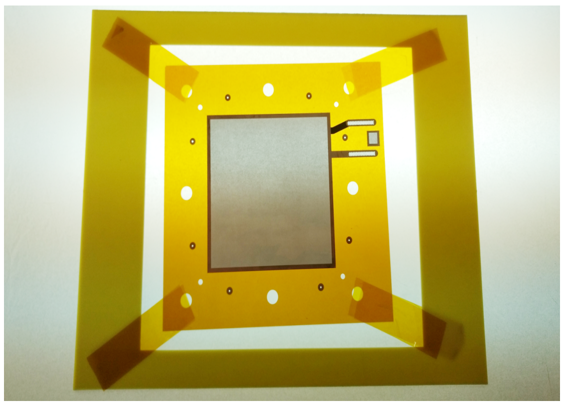

A newly produced
10 cm x 10 cm GEM foil

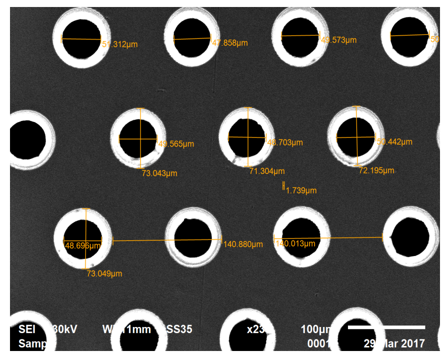

SEM images at µm level resolution

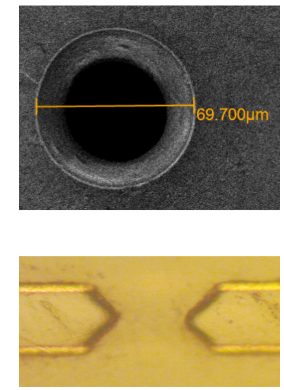

Single-hole structure

- Hole size and uniformity is very important as it describes the properties of the GEM detectors realized from these foils
- Qualification?

Qualification: QC Assessment

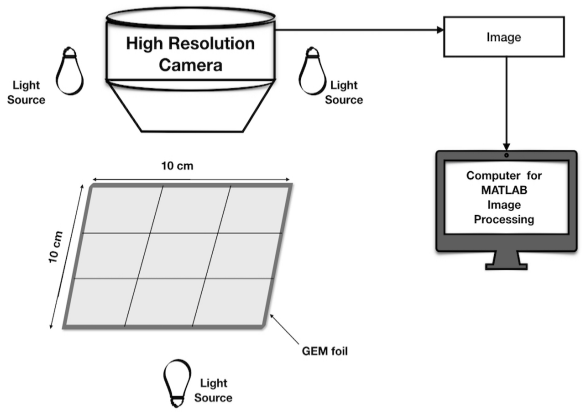

Optical assessment

- Foils scanned using Micro lensing technique
- Imperfections that have been observed are un-etched areas, under-size hole, oversize holes, without hole areas, excess etching, etc
- The hole diameters 49.9 µm and 70.01 µm for inner and outer holes
- Less than 0.15% of defects were observed

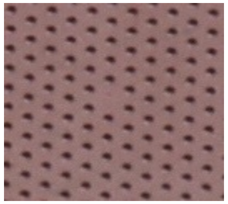

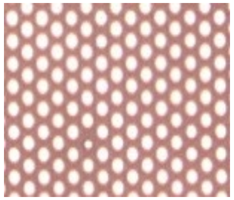

Electrical assessment

- Current of < 1 nA observed, which is consistent with CERN GEM foils
- No discharges has been observed at 550 V, and either a single or no discharge has been observed at 600

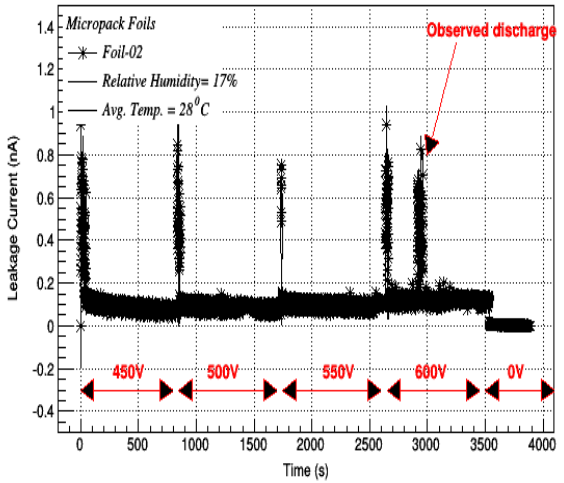

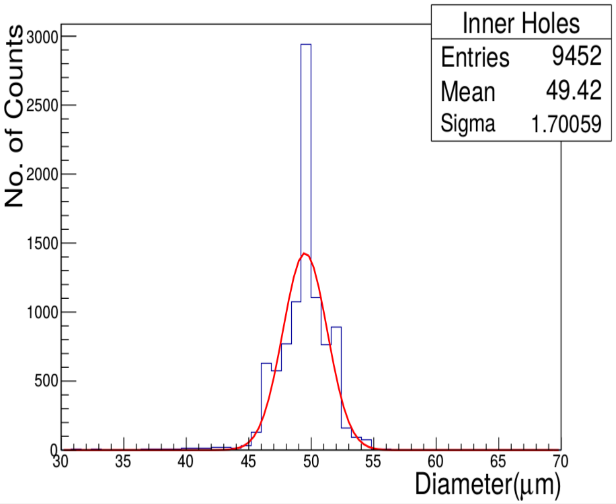

Hole diameters 49.9 µm

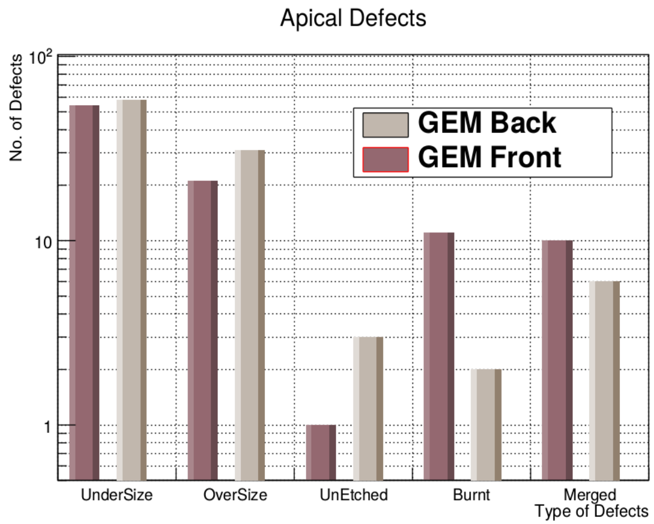

Performance of Indian made GEM foils

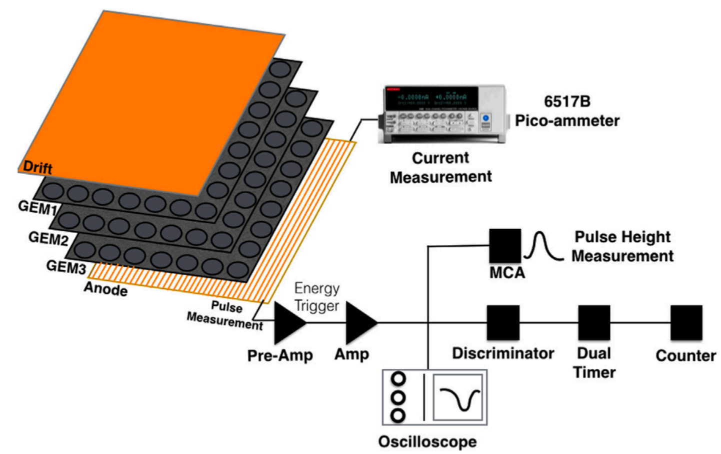

Fig. 3. Schematic of the set-up used for various studies using 10 cm × 10 cm triple GEM detector prototype.

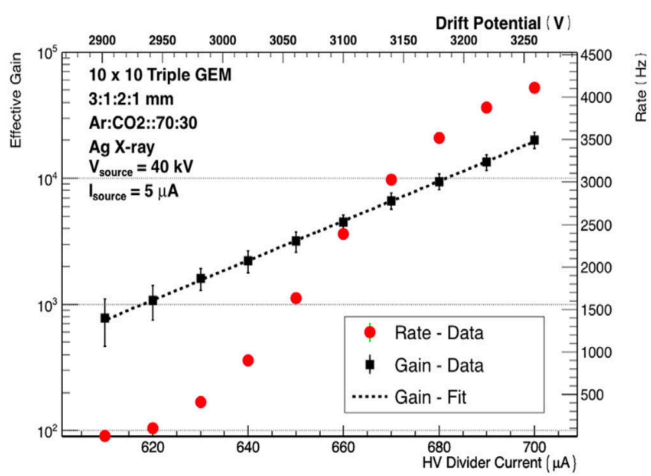

Nuclear Inst. and Methods in Physics Research, A 892 (2018) 10–17

Contents lists available at ScienceDirect

Nuclear Inst. and Methods in Physics Research, A

journal homepage: www.elsevier.com/locate/nima

Technical Notes

Development, characterization and qualification of first GEM foils produced in India

Aashaq Shah [a], Asar Ahmed [a], Mohit Gola [a], Ram Krishna Sharma [a,*], Shivali Malhotra [a], Ashok Kumar [a], Md. Naimuddin [a], Pradeep Menon [b], K. Srinivasan [b]

[a] Department of Physics & Astrophysics, University of Delhi, Delhi, India
[b] Micropack Pvt. Ltd., Bengaluru, India

ARTICLE INFO

Keywords:
GEM
Single-mask
Double-mask

ABSTRACT

The increasing demand for Gas Electron Multiplier (GEM) foils has been driven by their application in many current and proposed high-energy physics experiments. Micropack, a Bengaluru-based company, has established and commercialized GEM foils for the first time in India. Micropack used the double-mask etching technique to successfully produce 10 cm × 10 cm GEM foil. In this paper, we report on the development as well as the geometrical and electrical properties of these foils, including the size uniformity of the holes and leakage current measurements. Our characterization studies show that the foils are of good quality and satisfy all the necessary quality control criteria.

Nuclear Inst. and Methods in Physics Research, A 951 (2020) 162967

Contents lists available at ScienceDirect

Nuclear Inst. and Methods in Physics Research, A

journal homepage: www.elsevier.com/locate/nima

Performance of the triple GEM detector built using commercially manufactured GEM foils in India

Mohit Gola, Shivali Malhotra *, Aashaq Shah, Asar Ahmed, Ashok Kumar, Md. Naimuddin

Department of Physics & Astrophysics, University of Delhi, Delhi, India

ARTICLE INFO

Keywords:
Gaseous detector
Triple GEM
Characteristics

ABSTRACT

The Gas Electron Multiplier (GEM) detectors has been utilized for various applications due to their excellent spatial resolution, high rate capabilities and flexibility in design. The GEM detectors stand as a promising device to be used in nuclear and particle physics experiments. Many future experiments and upgrades are looking forward to use this technology leading to high demand of GEM foils. Until now, CERN is the only reliable manufacturer and distributor of GEM foils, but with technology transfer, few other industries across the globe have started manufacturing these foils employing the same photo-lithographic technique. The Micropack Pvt. Ltd. is one such industry in India which produced first few 10 cm × 10 cm GEM foils, which were then distributed to few collaborating partners for testing reliability and performance of foils before they can be accepted by the scientific community. Characterization of three such foils have already been performed by studying their optical and electrical properties. Using these foils a triple GEM detector has been built and various performance characteristics have been measured. In this paper, we specifically report measurements on gain, resolution and response uniformity, by utilizing local quality control set-ups existing at University of Delhi.

- Large size 30 cm x 30 cm developed
- The CMS size foils have been recently developed
- To plan for GE2/1, ME0 Indian made detectors

…. 2 more

For GE1/1 project, all DB and RB (~300 boards) used by CMS were Indian made

Medical Imaging with Indian GEM foils

- A triple-GEM detector utilizing Micropack foils were assembled and integrated with 2D readout board
- Image was reconstructed utilizing 2D information: GEMROC 64-channel chip

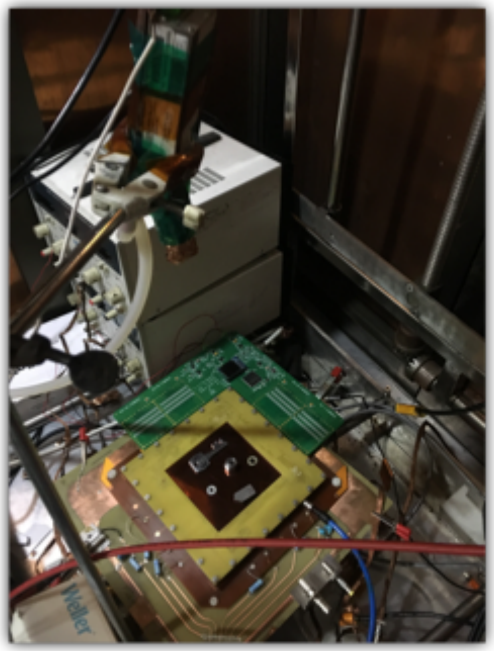

Imaging setup at Delhi University

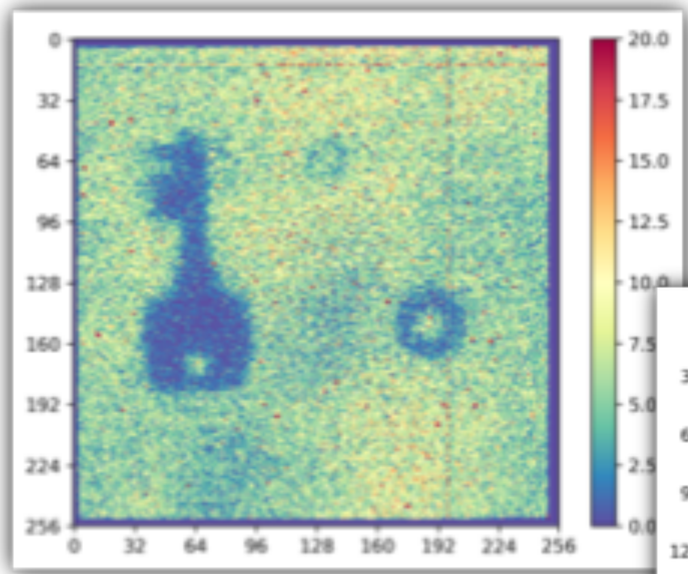

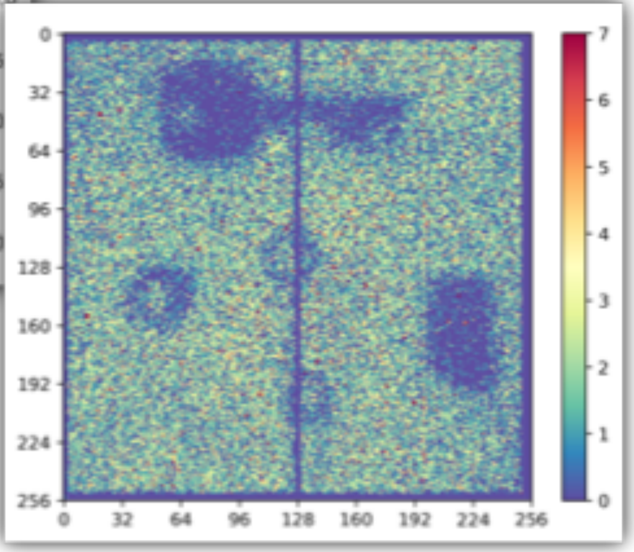

- The detector used under the operation was built using the Indian made GEM foils
- The detector was operated at a gain of 1000 under Ar/CO2:70/30

Part III: Physics Studies

Search for exotic Higgs boson decay in $h \to aa \to bb\mu\mu$

- The subject of exotic Higgs decays is not a new one
- Higgs boson has been discovered and mass is known at least
- We also know that its branching fraction into exotic states cannot exceed ≈ 50% [1]
- The question is: for various exotic final states
    - What branching fractions can be probed at the LHC?
    - How can the sensitivity to these final states be maximized?

[1] Phy. Rev. D 90, 075004 (2014), Revised on Oct 17, arXiv:1312.4992

Motivation (1/1)

Why $bb\mu\mu$ final state?

- **Part of the work dedicated to muon upgrade**
  - **Natural to choose a final state having muons**

- **$h \rightarrow X_1X_2 \rightarrow 4\mu$:**
  - **Cleaner but very rare**

- **$h \rightarrow X_1X_2 \rightarrow 4b$:**

  Expected to occur with more number of events but has challenging backgrounds

- **$h \rightarrow X_1X_2 \rightarrow bb\mu\mu$ Scenario:**
  - **Compromise between the channels with 4b and 4μ final states**
  - **Very attractive for discovering SM extensions with extra singlets**
    - **$a \rightarrow \mu\mu$ has a clear peak with controlled backgrounds**
    - **$a \rightarrow bb$: large BR in many parts of the parameter space**
    - **Expected to provide better sensitivity in the long run and the best discovery avenue for many BSM models [1, 2]**

○ A promising search channel for $h \rightarrow aa \rightarrow bb\mu\mu$

relatively large branching ratio, moderate background

[1] Phy. Rev. D 90, 075004 (2014)
[2] JHEP 1308 (2013) 019, [arXiv:1303.2113]

Motivation (1/2)

E-mail: dcurtin1@umd.edu, rouven.essig@stonybrook.edu,
yiming.zhong@stonybrook.edu

ABSTRACT: The search for exotic Higgs decays are an essential probe of new physics. In particular, the small width of the Higgs boson makes its decay uniquely sensitive to the existence of light hidden sectors. Here we assess the potential of an exotic Higgs decay search for $h \to 2X \to b\bar{b}\mu^+\mu^-$ to constrain theories with light CP-even ($X = s$) and CP-odd ($X = a$) singlet scalars in the mass range of 15 to 60 GeV. This decay channel arises naturally in many scenarios, such as the Standard Model augmented with a singlet, the two-Higgs-doublet model with a singlet (2HDM+S) — which includes the Next-to-Minimal Supersymmetric Standard Model (NMSSM) — and in hidden valley models. The $2b2\mu$ channel may represent the best discovery avenue for many models. It has competitive reach, and is less reliant on low-p_T b- and τ-reconstruction compared to other channels like $4b$, 4τ, and $2\tau 2\mu$. We analyze the sensitivity of a $2b2\mu$ search for the 8 and 14 TeV LHC, including

JHEP 06 (2015) 025

nuons leads to very hierarchical branching ratios,

$$\iota \to 4\mu) = \frac{\varepsilon}{2}\mathrm{Br}(h \to 2b2\mu) = \varepsilon^2 \mathrm{Br}(h \to 4b), \tag{72}$$

$\mathrm{Br}(a \to b\bar{b}) \sim m_\mu^2/3m_b^2 \approx 2 \times 10^{-4}$ in the SM+S. (Non-minimal this ratio, but the ratio is in general very small.) Assuming SM Higgs production and $\mathrm{Br}(h \to aa) = 10\%$ leads to zero $h \to 2a \to 4\mu$ events from gluon fusion at LHC Run I, while about twenty $h \to 2a \to 2b2\mu$ events are expected to occur. Even though this is much less than the few hundred $h \to 2a \to 4b$ events expected from associated production, the backgrounds for the $4b$ search are so challenging (see §3) that the $2b2\mu$ channel may provide much better sensitivity. This is even more attractive in non-minimal models, where e.g. $\tan\beta$ can enhance the leptonic pseudoscalar branching fraction significantly. It is also possible that the Higgs decays to two pseudo scalars, $h \to a_1 a_2$, which have large branching fractions to $2b$ and 2μ, respectively. The presence of a clean dimuon resonance makes the $2b2\mu$ decay mode very attractive for discovering SM extensions with extra singlets.

Phy. Rev. D 90, 075004 (2014) and arXiv:1312.4992v6 [hep-ph] 9 Oct 2017

Optimization

- **Model Used**
  - ● **NMSSMHET used in MadGraph_aMCatNLO, generated signal at LO Mechanism**
  - ● **Mechanism**
    - **ggF with σ_{ggF} = 48.58 pb**
    - **VBF with σ_{VBF} = 3.78 pb**
- **Benchmark for the expected yield**
  - **BR($h \rightarrow aa$) = 10% and BR($aa \rightarrow \mu\mu bb$) = 1.7×10^{-3}**
  - **2HDM+S Type 3, tan(β)=2.0 for a→ff**

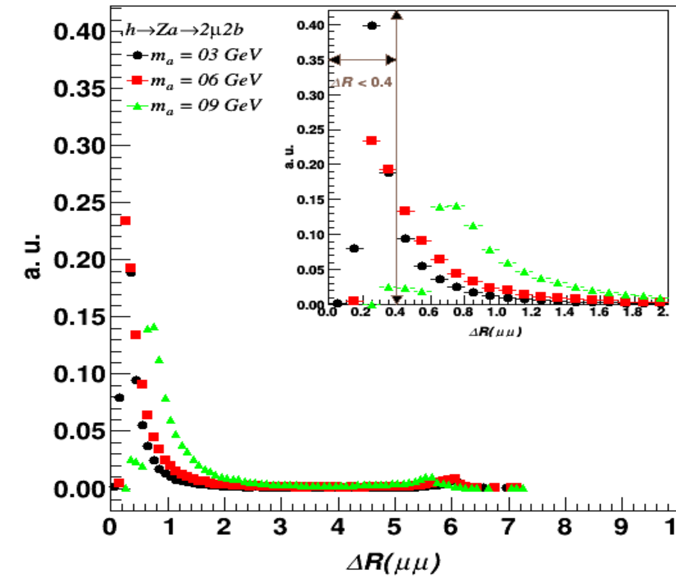

- **Selecting mass window**
  $h \rightarrow aa \rightarrow 2b2\mu$ (1 GeV to 62.5 GeV)
  - **Below 20 GeV jets are collimated**
  - **Explore generator level information**
  - **Analysis uses ΔR = 0.4 and check it between pair of μ's**
  - **Below 20 GeV, analysis needs to changed**
  - **Selected a mass window 20 < $m_{\mu\mu}$ < 62.5 GeV**

Reconstructed mass of pair of b-jets

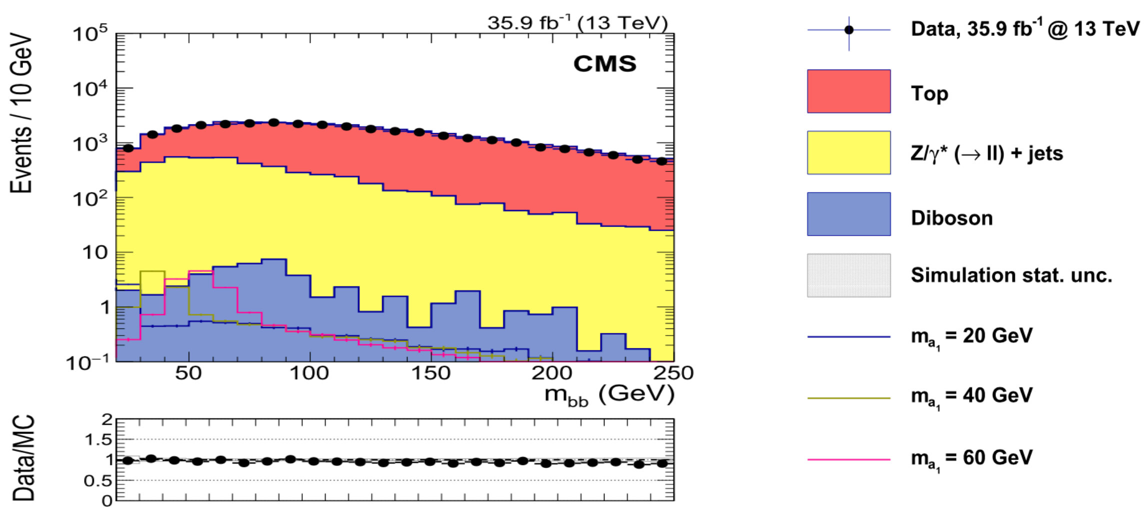

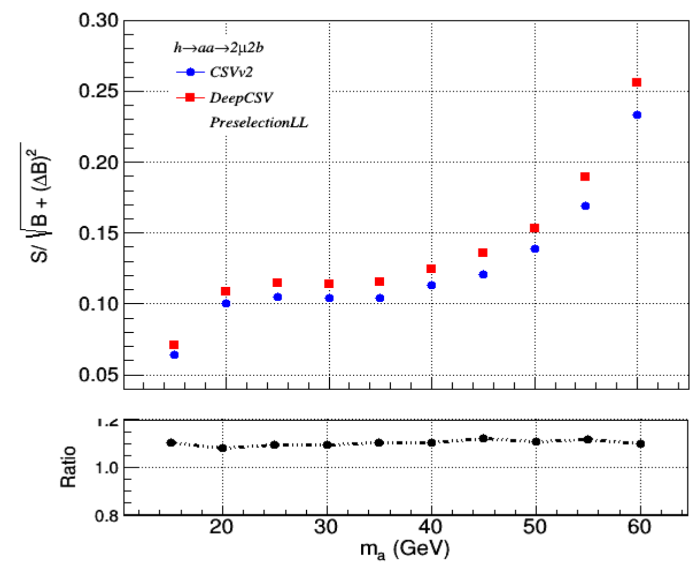

Reducing backgrounds

- **Based on Chi Square (χ^2)**
  - **Exploit features and define as χ^2**
    - **For h→aa→bbμμ**

$$\chi^2 = \chi^2_{b\bar{b}} + \chi^2_h$$

$$\chi_{b\bar{b}} = \frac{(m_{b\bar{b}} - m_{\mu^-\mu^+})}{\sigma_{b\bar{b}}} \quad and \quad \chi_h = \frac{(m_{b\bar{b}\mu^-\mu^+} - m_h)}{\sigma_h}$$

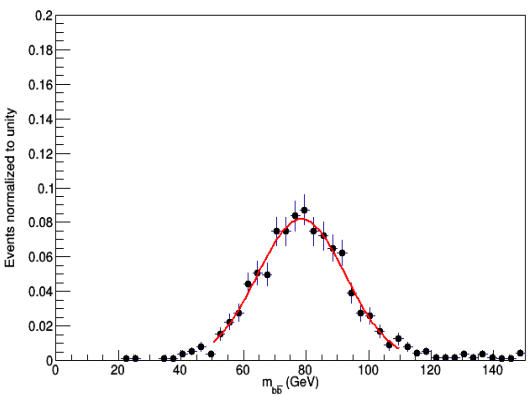

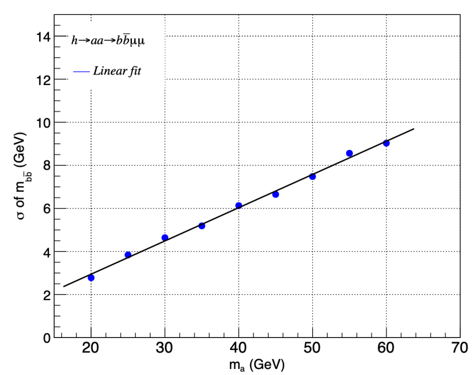

- **Contour of radius less than 5 (i.e., χ^2 < 5) is defined as the signal region**

- **This selection has efficiency up to ≈ 40-45% for signal while rejecting over 95% of the background events**

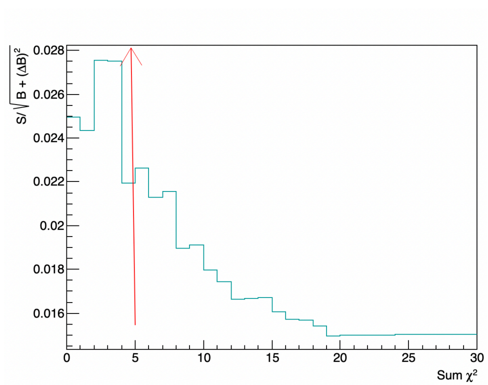

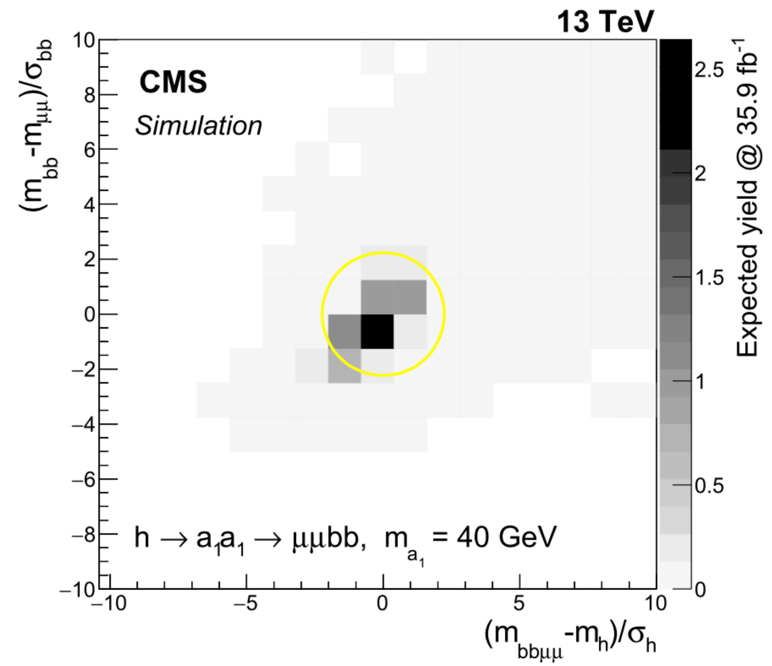

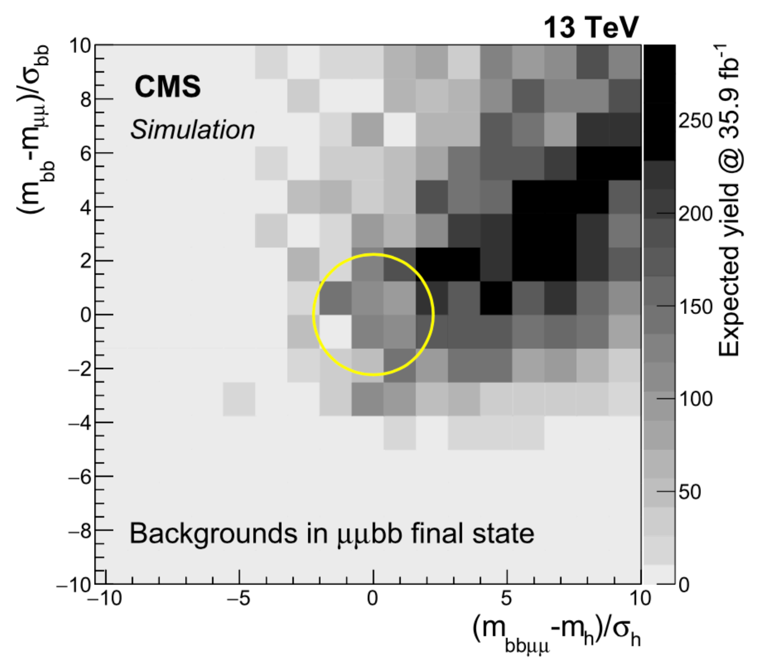

Signal Modelling

- **Signal Shape derived from simulation**
- **Combination of Voigtion and a Crystal ball profiles**
- **Established a 3-parameter model**

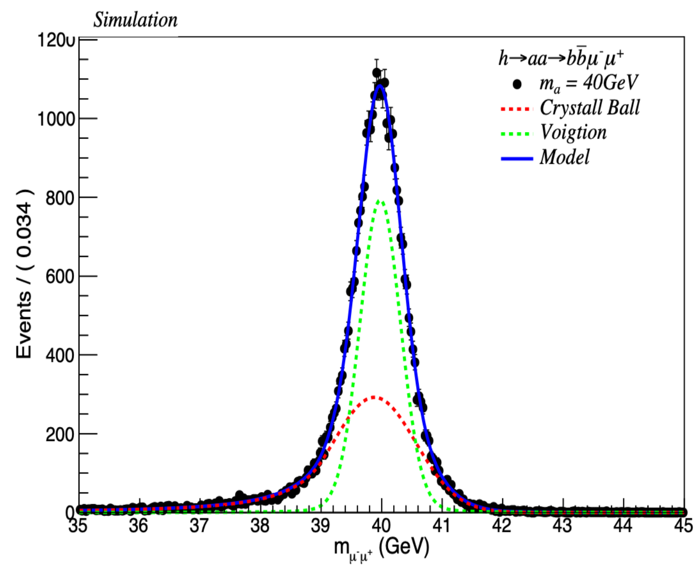

Signal model

$$S(m_{\mu^-\mu^+} \mid f, p_V, p_{CB}) \equiv f \cdot V(m_{\mu^-\mu^+} \mid p_V) + (1-f) \cdot CB(m_{\mu^-\mu^+} | p_{CB})$$

Voigt function

$$\begin{aligned} V(m_{\mu^-\mu^+} \mid p_V) &\equiv V(m_{\mu^-\mu^+}, \sigma, \gamma, m_a) = G(m_{\mu^-\mu^+}, \sigma, m_a) * L(m_{\mu^-\mu^+}, \gamma, m_a) \\ &= \left(\frac{e^{-(m_{\mu^-\mu^+} - m_a)^2/2\sigma^2}}{\sigma\sqrt{2\pi}} \right) * \left(\frac{\gamma}{\pi((m_{\mu^-\mu^+} - m_a)^2) + \gamma^2} \right) \end{aligned}$$

Crystal ball function

$$CB(m_{\mu^-\mu^+}, n, \sigma_{CB}, \alpha, m_a) = N \cdot \begin{cases} e^{-(m_{\mu^-\mu^+} - m_a)^2/2\sigma_{CB}^2}, & \text{for} \frac{m_{\mu^-\mu^+} - m_a}{\sigma_{CB}} > -\alpha \\ A \cdot \left(B - \frac{(m_{\mu^-\mu^+} - \mu_a)}{\sigma_{CB}} \right)^{-n} & \text{for} \frac{m_{\mu^-\mu^+} - m_a}{\sigma_{CB}} \leq -\alpha \end{cases}$$

Background Model

- **A fully data driven approach using MultiPdf is employed**

- **Data is modeled with different functions with different degrees**
    - **Polynomials**
    - **Inverse polynomials**
    - **Chebychev**
    - **Bernstein functions**

- **An F-test is used to determine the collection of pdfs**
- **The lowest degree where the χ^2 /ndf**

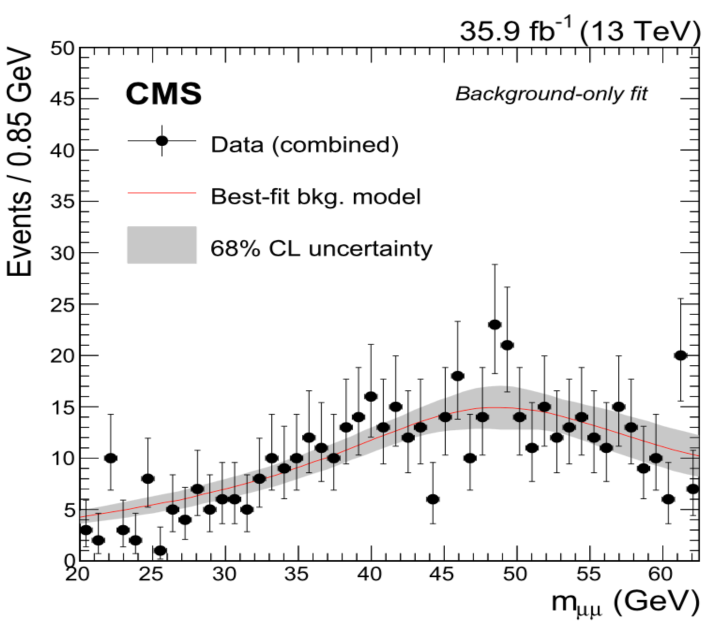

[1] Phy. Lett. B. 795 (2019) 398

Tight-Loose (TL) category			
Model	χ^2/ndf	F-test probability (> 0.05)	Decision
Polynomial I	1.16	-	✓
Polynomial II	1.09	0.10	✓
Polynomial III	1.03	0.25	✓
Polynomial IV	1.01	0.91	✓
Inv. Poly I	1.15	-	✓
Inv. Poly II	1.07	0.16	✓
Inv. Poly III	1.03	0.01	×

Table 6: Trial functions with different orders are selected to model the background in TL category depending upon the outcome of the F-test. The pdf's marked with '†' sign are not selected as they are repeating in another polynomial category.

Tight-Loose (TL) category			
Model	χ^2/ndf	F-test probability (> 0.05)	Decision
Bernstein II	1.13	-	✓
Chebychev I†	1.16	-	×
Chebychev II	1.06	0.10	✓
Chebychev III	1.02	0.25	✓
Chebychev IV	1.00	0.60	✓

Table 7: Trial functions with different orders are selected to model the background in TL category depending upon the outcome of the F-test. The pdf's marked with '†' sign are not selected as they were repeating in another polynomial category.

Results

- No significant excess of events over the SM background prediction
- The limits on the branching ratio are (1–6) $\times 10^{-4}$
- Improved results w.r.t Run-I by a factor of 1.4-1.8
- 20% more sensitivity compared to ATLAS
- Results with 2017 data are even more improved because of analysis strategies and the use of new b-tagging algorithms

Phys. Lett. B 795 (2019) 398

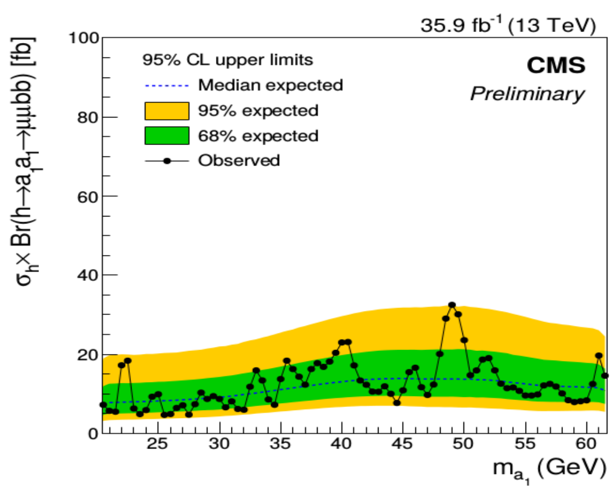

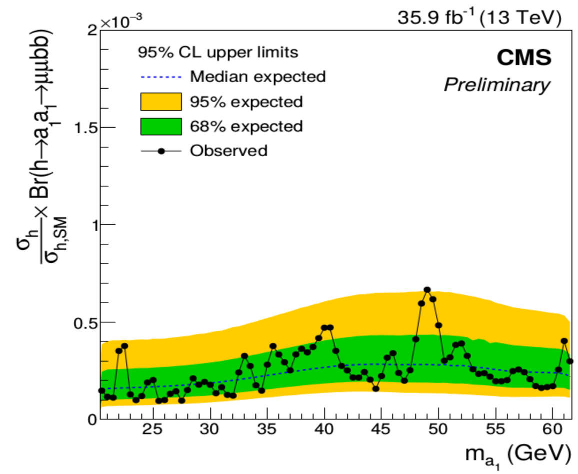

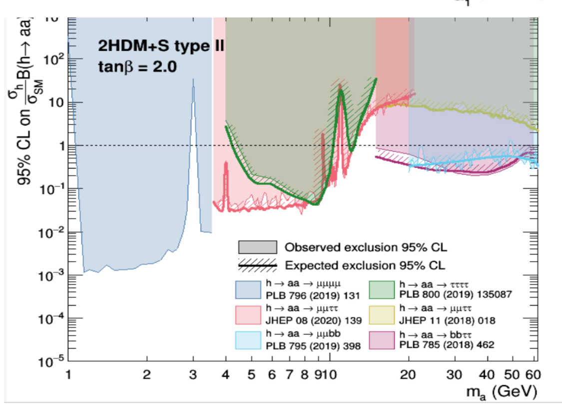

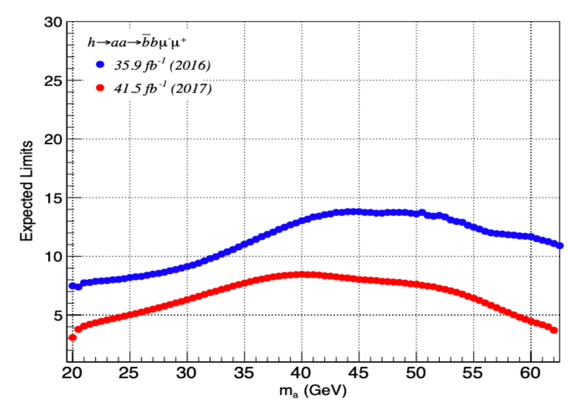

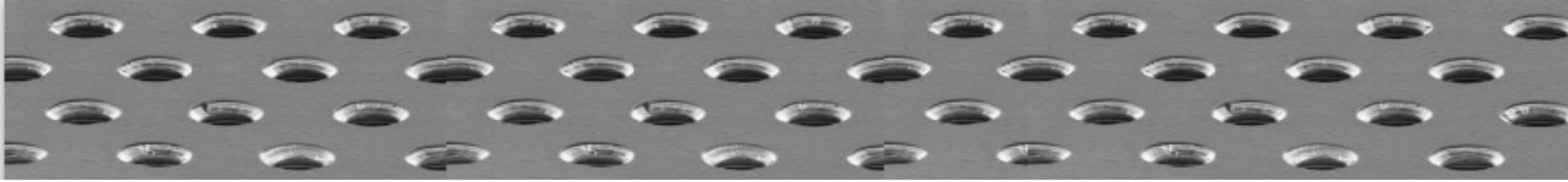

GE1/1 design and Assembly

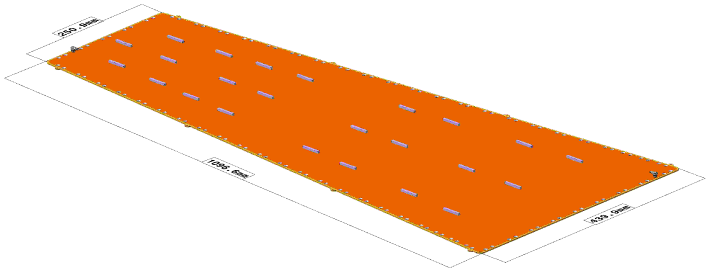

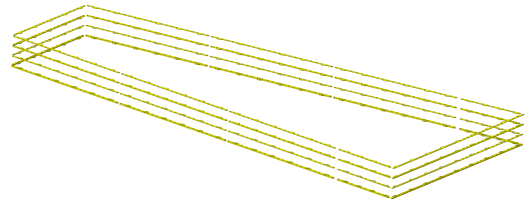

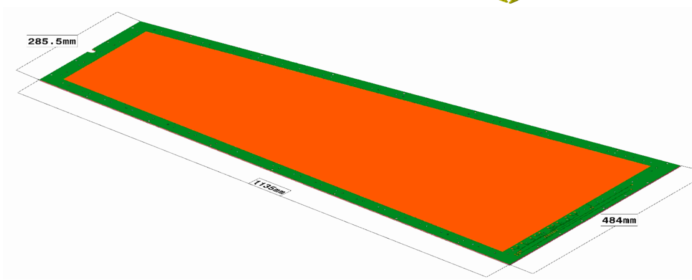

- Assembly of GE1/1 detectors takes place in a clean room of Class 1000
- The procedure starts with the preparation of the drift board, followed by the assembly of the GEM stack and finally closure of the detector
- Initially, thermal stretching was used
  Time consuming and laborious
- GEM foils are mechanically stretched
- The stack is then uniformly stretched against the pull-outs by applying a controlled torque of about 8-10 cNm on the lateral screws, pulling the inner frame out-wards towards the pull-outs

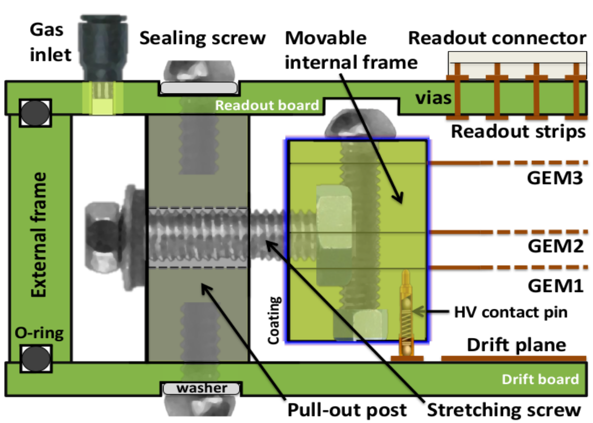

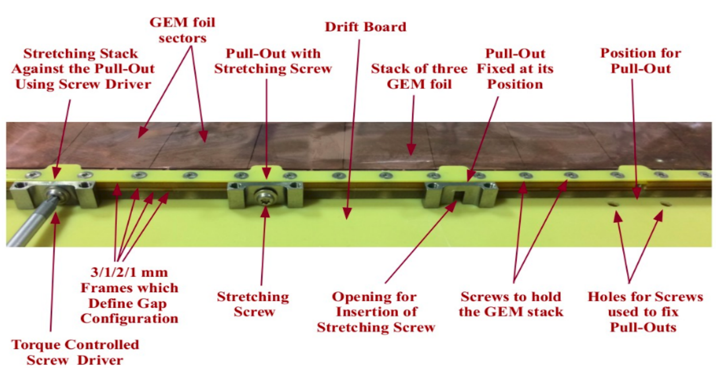

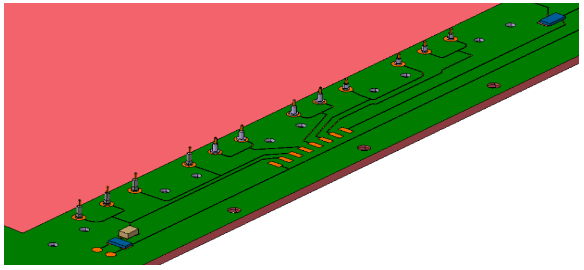

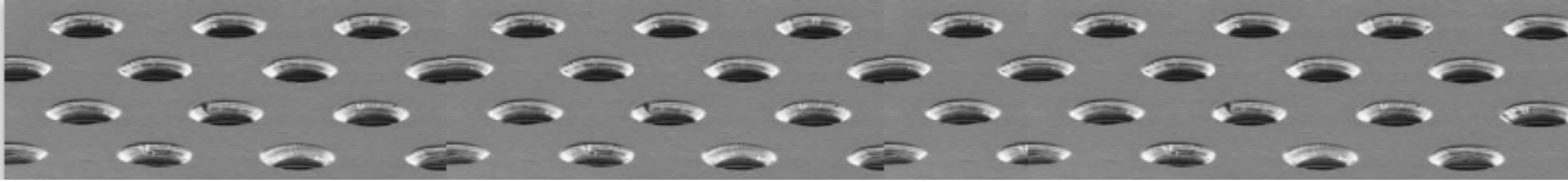

Uniformity in Resolution

- The measurements performed at equal electrical field (drift, transfer-1, transfer-2 and induction field) configurations
- Energy resolution of each sector was measured
- The energy resolution over the active area varies from 18% to 22% in ‘Orientation A’ and 24% to 28% in ‘Orientation B’.

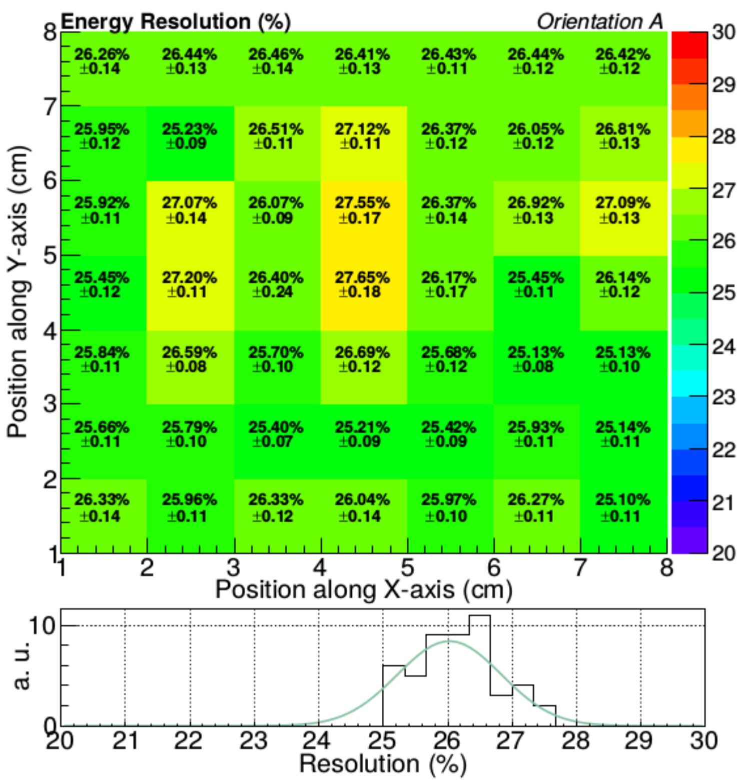

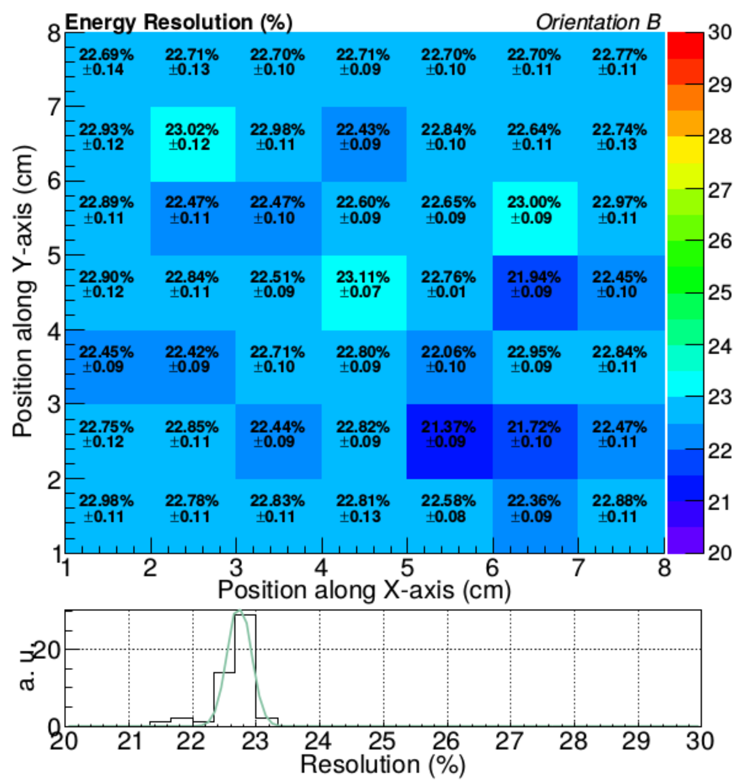

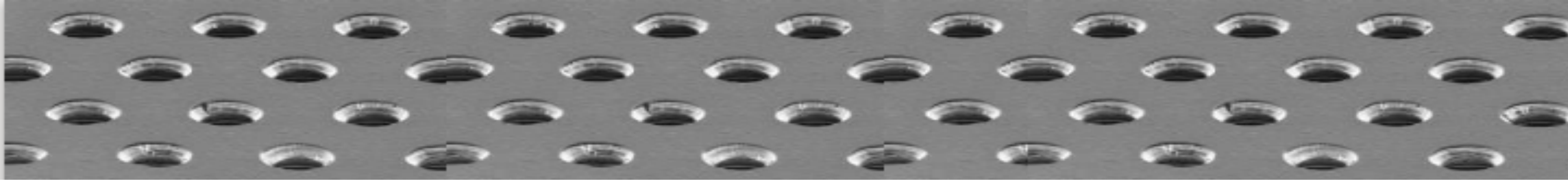

Commitment from Delhi University (DU) GEM group

- GE/1 chamber production and validation is really complex. Therefore, several assembly lines have were established in parallel to perform mass production
    - FIT (USA), INFN (Italy), DESY (Germany) and DU (India), etc.

- Delhi University has been involved in the GE1/1 upgrade projects at many fronts:
    - R&D both at CERN and Delhi
    - Chamber production, QC and validation
    - Several chambers validated at CERN

- Eight full-size GE1/1 chambers have been assembled in 2018

- Quality Control (QC) tests were performed
  QC2, QC3, QC4, QC4, QC5 (I and II)

- All the eight chambers were validated and shipped to CERN

- RO and DB are manufactured by Micropack (Bangluru) and are shipped to CERN

A photograph of a shipment box at DU containing six GE1/1 chambers waiting to be shipped to CERN (August, 2018)

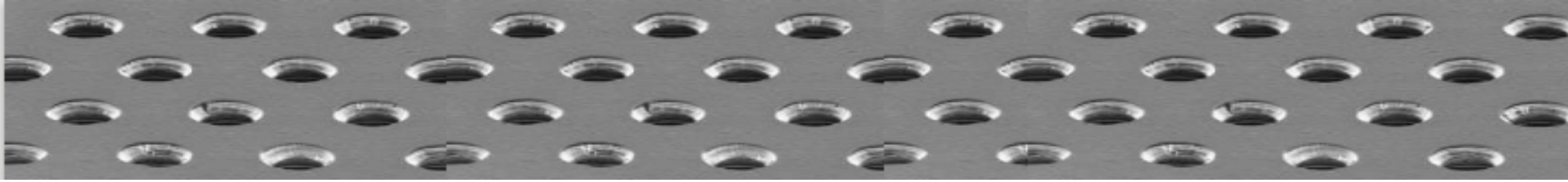

Model		$m_a \in [1, 3.5]$ GeV	$m_a \in [5, 15]$ GeV	$m_a \in [20, 62.5]$ GeV
	$\mathcal{B}(a \to \mu^-\mu^+)$	$4.6 \times 10^{-3} - 4.0 \times 10^{-2}$	$2.1 \times 10^{-4} - 1.8 \times 10^{-3}$	$2.0 \times 10^{-4} - 2.2 \times 10^{-4}$
Type-1	$\mathcal{B}(a \to \tau^-\tau^+)$	0	$5.7 \times 10^{-2} - 3.6 \times 10^{-1}$	$5.5 \times 10^{-2} - 6.3 \times 10^{-2}$
	$\mathcal{B}(a \to b\bar{b})$	0	–	$8.3 \times 10^{-1} - 8.8 \times 10^{-1}$
	$\mathcal{B}(a \to \mu^-\mu^+)$	$2.5 \times 10^{-2} - 3.8 \times 10^{-2}$	$2.2 \times 10^{-4} - 4.0 \times 10^{-3}$	$2.1 \times 10^{-4} - 2.5 \times 10^{-4}$
Type-2	$\mathcal{B}(a \to \tau^-\tau^+)$	0	$6.0 \times 10^{-2} - 7.9 \times 10^{-1}$	$5.8 \times 10^{-2} - 7.0 \times 10^{-2}$
$\tan\beta = 2$	$\mathcal{B}(a \to b\bar{b})$	0	–	$9.2 \times 10^{-1} - 9.3 \times 10^{-1}$
	$\mathcal{B}(a \to \mu^-\mu^+)$	$7.4 \times 10^{-1} - 9.6 \times 10^{-1}$	$3.5 \times 10^{-3} - 5.0 \times 10^{-3}$	$3.4 \times 10^{-3} - 3.5 \times 10^{-3}$
Type-3	$\mathcal{B}(a \to \tau^-\tau^+)$	0	$9.1 \times 10^{-1} - 9.9 \times 10^{-1}$	9.7×10^{-1}
$\tan\beta = 5$	$\mathcal{B}(a \to b\bar{b})$	0	–	$2.0 \times 10^{-2} - 2.5 \times 10^{-2}$
	$\mathcal{B}(a \to \mu^-\mu^+)$	$4.5 \times 10^{-3} - 1.4 \times 10^{-1}$	$1.2 \times 10^{-3} - 1.8 \times 10^{-3}$	$1.1 \times 10^{-3} - 1.2 \times 10^{-3}$
Type-4	$\mathcal{B}(a \to \tau^-\tau^+)$	0	$3.2 \times 10^{-1} - 3.5 \times 10^{-1}$	$3.0 \times 10^{-1} - 3.3 \times 10^{-1}$
$\tan\beta = 0.5$	$\mathcal{B}(a \to b\bar{b})$	0	–	$2.5 \times 10^{-1} - 3.2 \times 10^{-1}$

Table 6.3: Branching fractions [11], as a function of the mass, of the pseudoscalar boson a to b quarks, τ leptons, and muons in the four different scenarios of 2HDM+S considered in Figure 6.1.

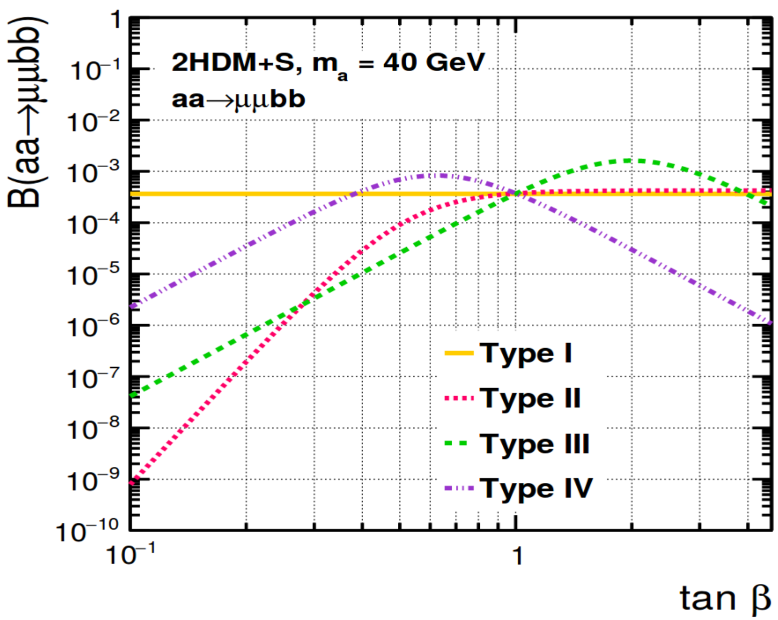

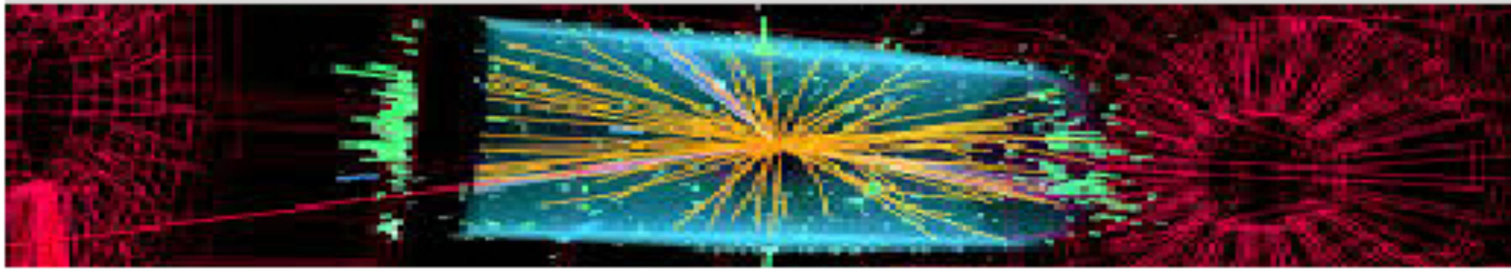

Systematic Uncertainities

Signal

Uncertainties on signal model parameters are found to be negligible

Signal normalization is affected by various sources of systematic uncertainties:

- Luminosity: ± 2.3%
- Pileup: ± 4.6% on the σ_{pp} inelastic
- μ ID, Iso, HLT scale factors: doubled for p_T < 20 GeV
- JES: p_T and η dependent corrections applied on jets and propagated to MET
- Unclustered energy
- b-tagging: different sources affecting the shape calibration are considered
- Automatically doubled for low p_T jets
- Uncertainties from JES and light flavor contamination in b-jet samples are the largest

Background

- Uncertainties on the background model are taken into account with the discrete profiling method

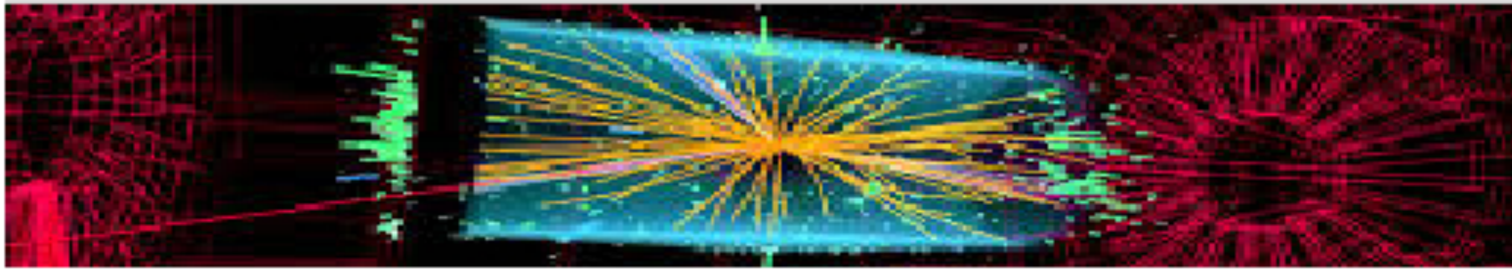

Background Model

- As mentioned previously, for $h \to aa \to \mu\mu bb$ we sub-categorize TL region in three regions based on b-tag working points
  - Control Region is fitted in different categories
  - TL category (One jet passes tight selection, and the other only passes loose selection and fails to pass medium and tight selection)
  - TM (One jet passes tight selection, and the other exclusively passes medium selection and fails tight selection)
  - TT (Both the jets pass tight selections)

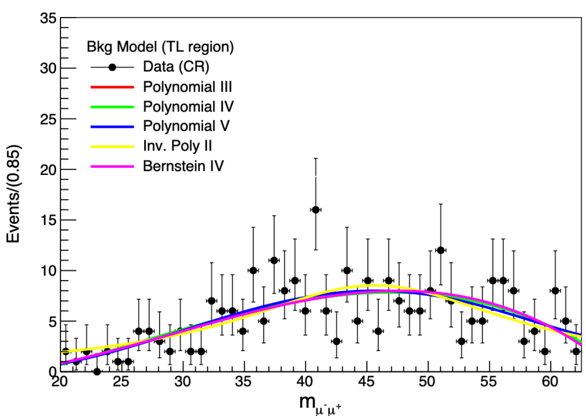

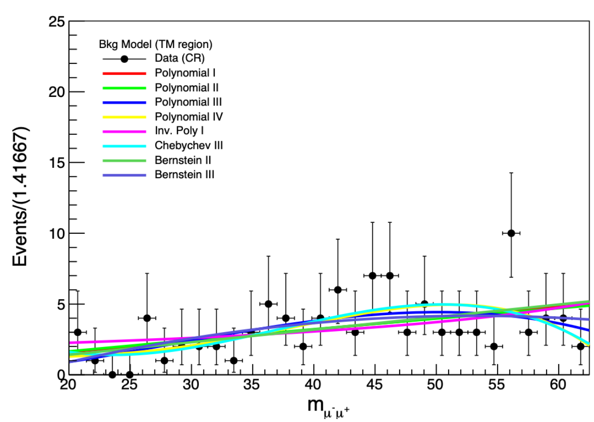

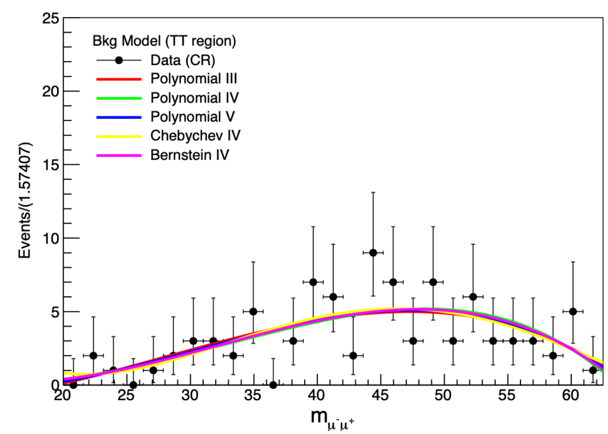

Expected limits have been calculated after combining all the three categories

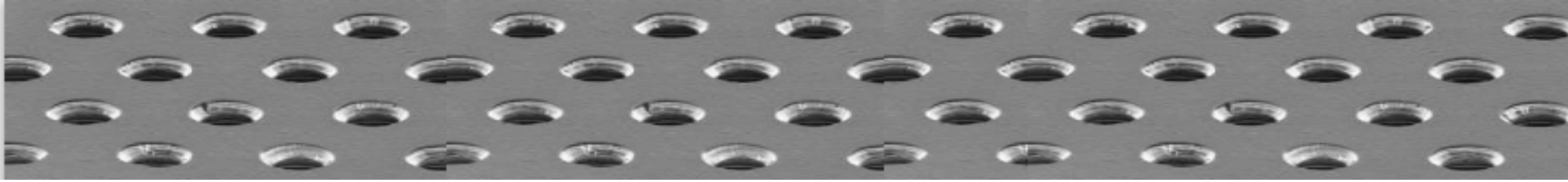

The CMS Muon Endcap Upgrade using GEM technology

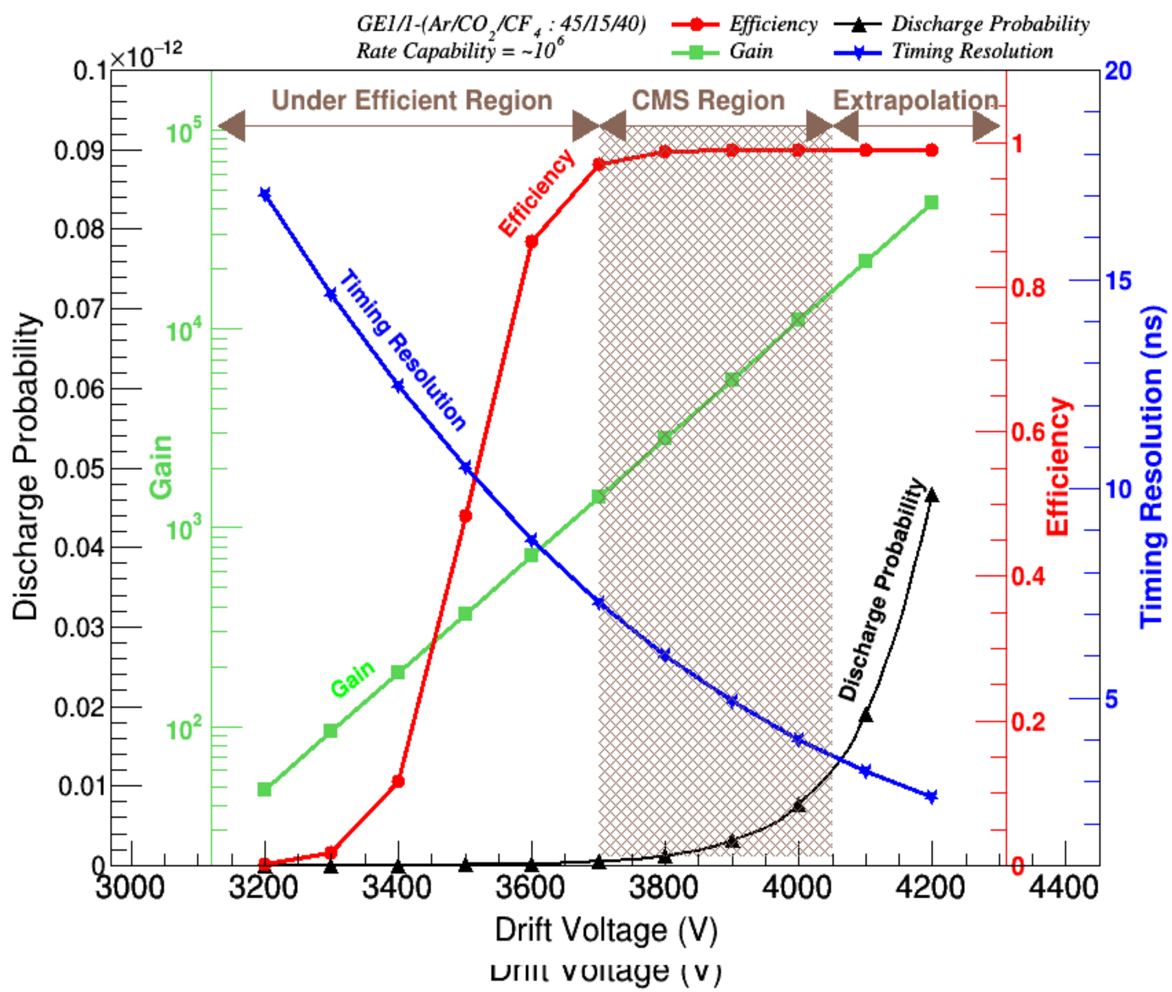

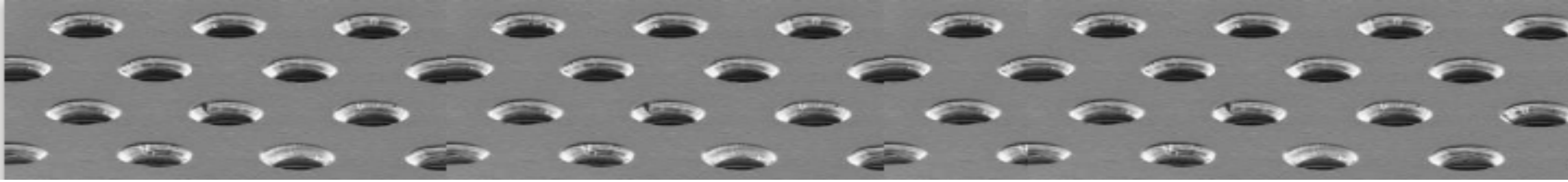

GE1/1 Performance: Gain Measurements

- The chamber is connected to the gas system and flushed with the gas mixture $Ar/CO_2/CF_4$ (45/15/40) at the flow rate of 5 L/hr
- The choice of using CF_4 quencher is driven by its good timing characteristics
- The effective gas gain is measured by exposing the detector to an X-ray source with a silver target for generating X-rays
- The gain is measured in by comparing the primary current I_p induced in the drift gap and the amplified output current (I_o) induced on the readout board
- The output current is measured using pico-ammeter connected to Keithley Electrometer Model 6487
- Data is recorded with a LabVIEW program

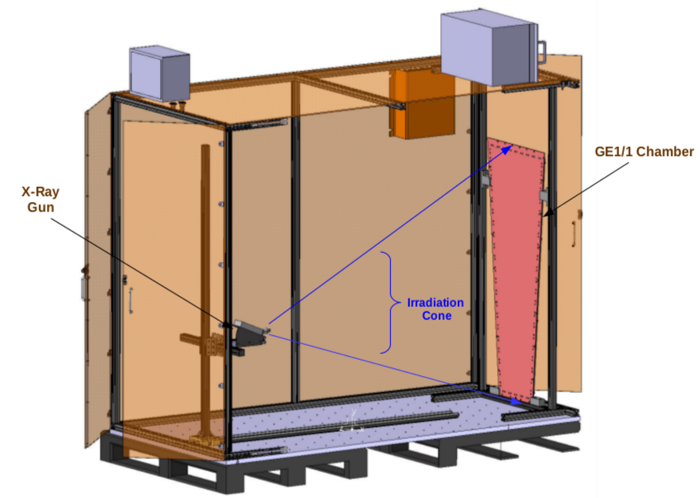

Design of the setup used for gain measurements with X-rays and the GE1/1 detector inside the copper chamber

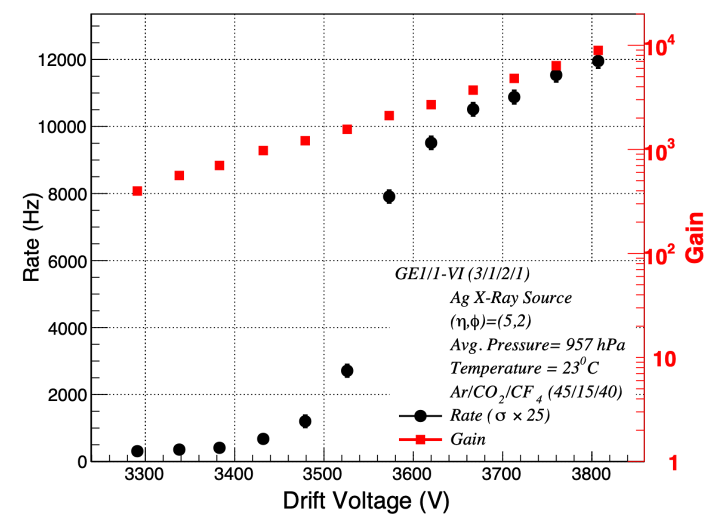

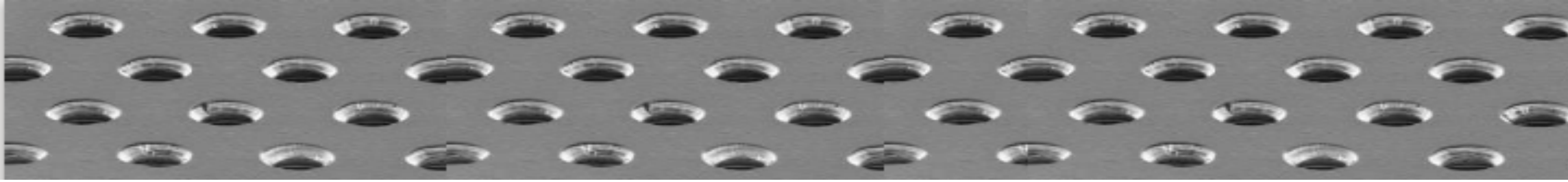

Pulse Height Spectrum

- Spectra taken after certain intervals of time when detector was placed under continuous irradiation (Fe-55)
- Shift in gain for Orientation A while no shift in Orientation B is observed
- Resolution measured after every minute at an initial gain of 2.2 X 10^4
- Effect is related to charging up behavior of the detector

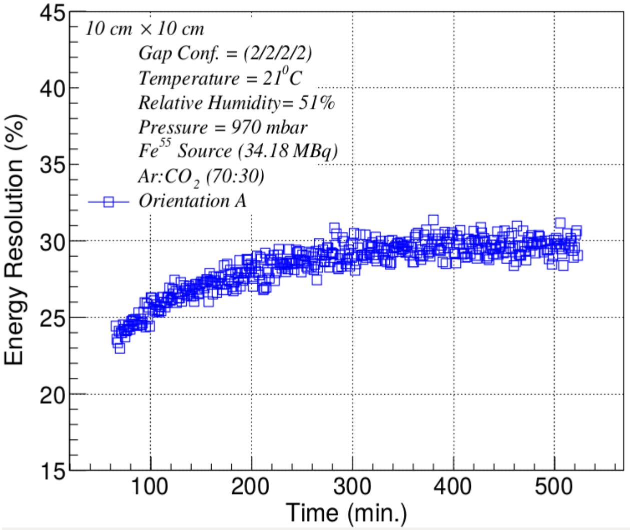

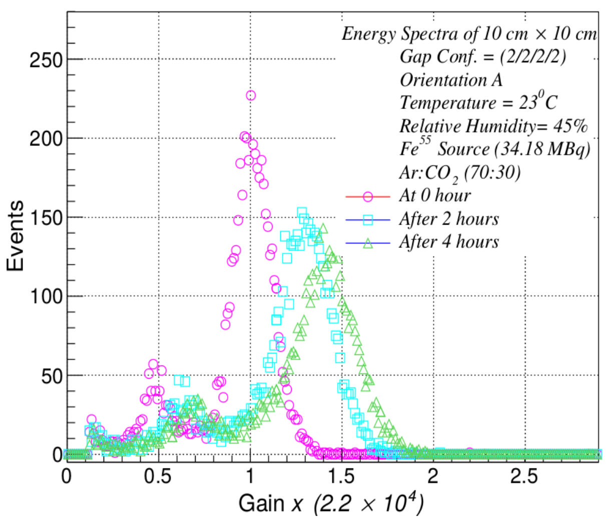

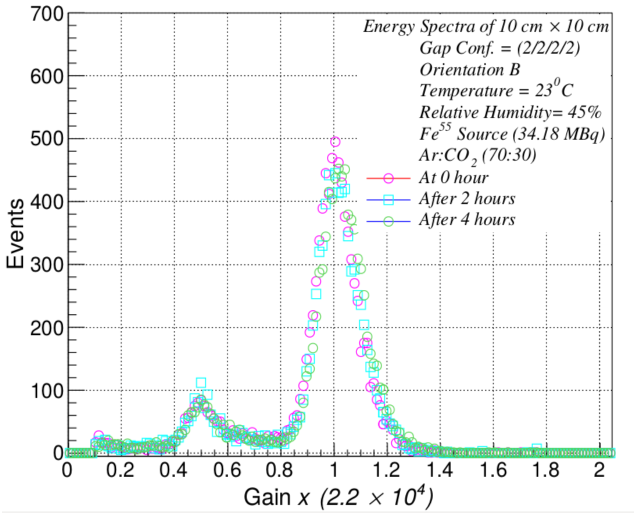

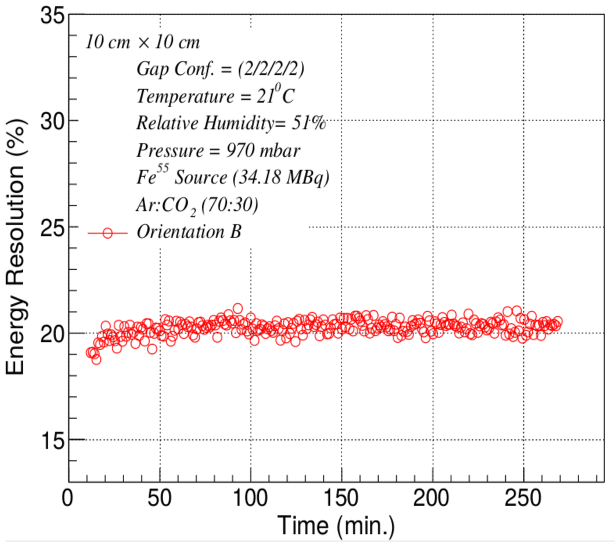

Charging Up Studies

- Charging-up takes place when one starts irradiating the detector
- Biconical Geometery, field lines hit the kapton surface
- More electrons/ions are collected on the kapton periphery
- Modify the ressulting field (increase)
- Increase the gain of the detector
- Local effect

Final distribution

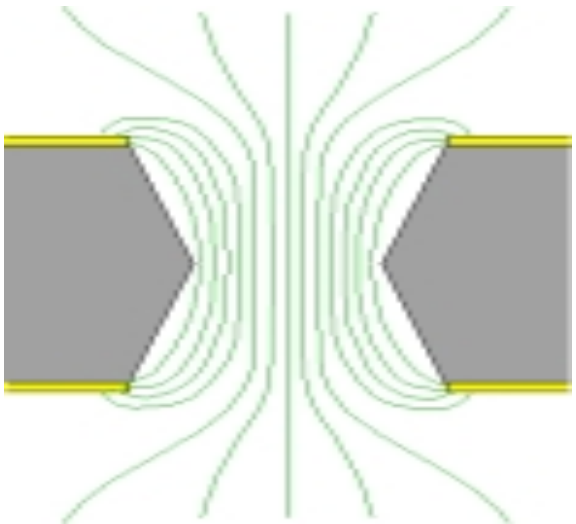

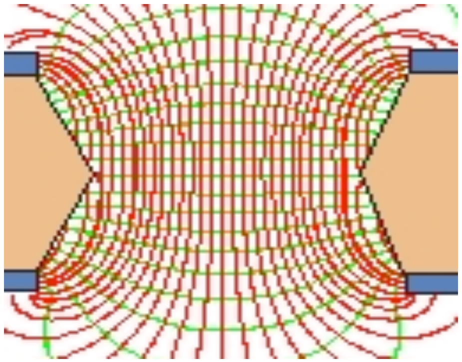

Field distribution

Biconical

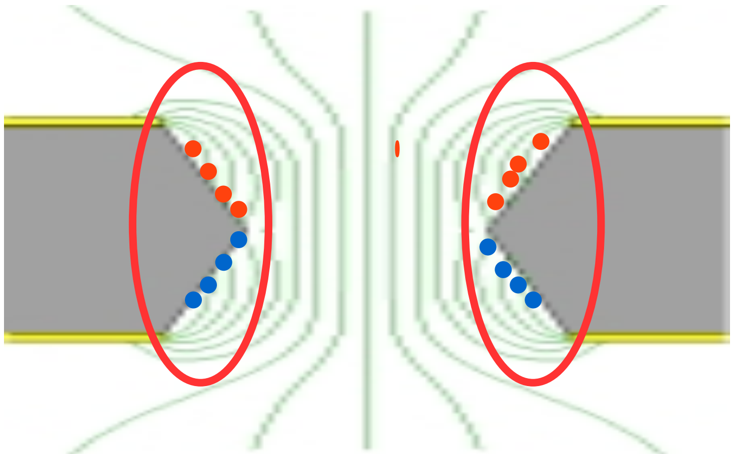

Conical

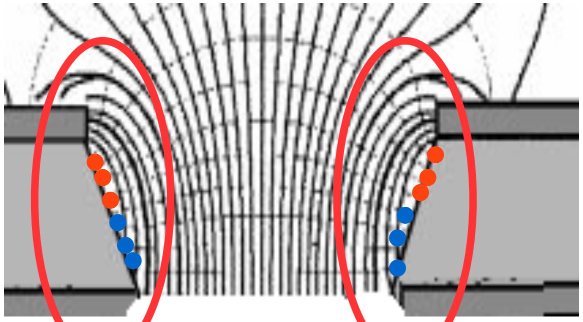

Cylindrical

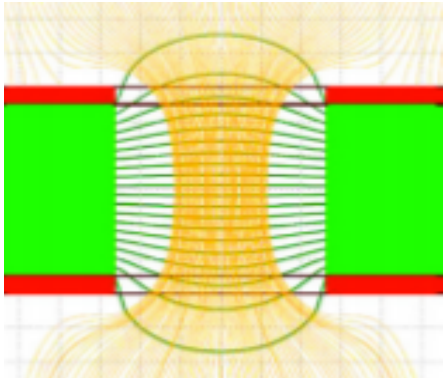

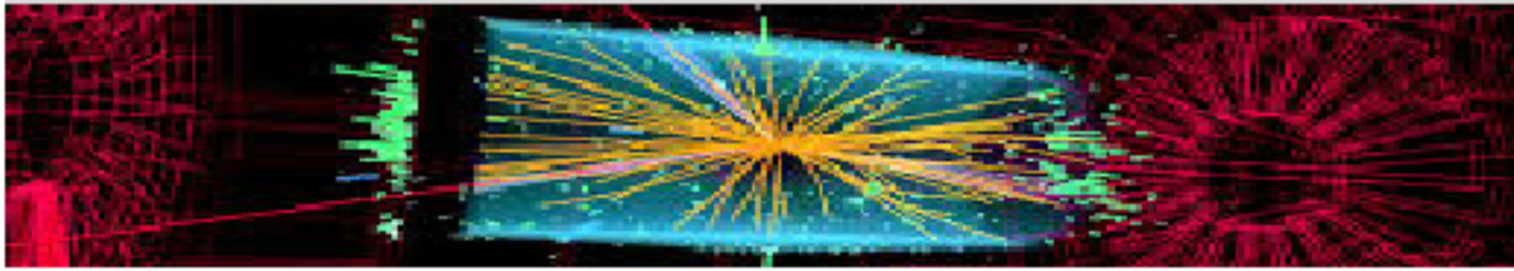

Optimization

- **Initially selected loose cuts on signal sample :**
  - **p_T^{μ} (leading/sub-leading) > 17, 8 GeV**
  - **p_T^{jet} (leading/sub-leading) > 10 GeV**
  - **both jets selected with loose b-tag discriminant**

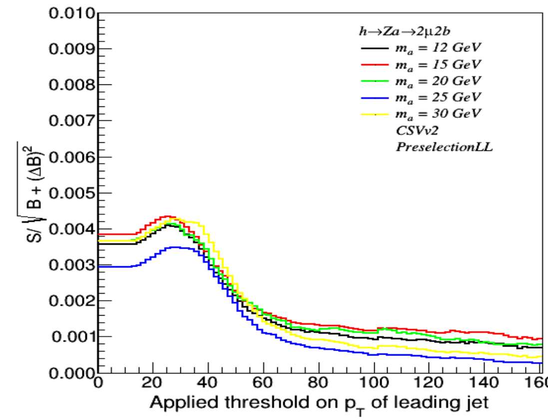

- **Variable $s/\sqrt{b+(\delta b)^2}$ used, where δb is the statistical uncertainty from MC**

- **Pair of jets in the final state:**
  1) **Loose-Loose (LL)**
  2) **Medium-Loose (ML)**
  3) **Tight-Loose (TL)**
  4) **Medium-Medium (MM)**
  5) **Tight-Medium (TM)**
  6) **Tight-Tight (TT)**

DeepCSV shows comparatively higher Significance than CSVv2

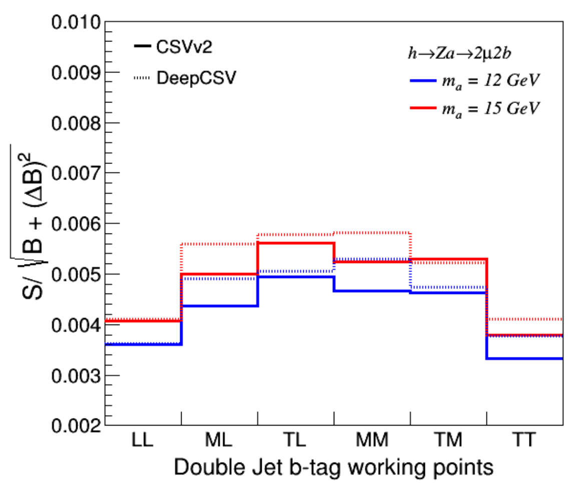

Based on μ-Isolation and ID

Tight Isolation-Medium ID is the optimal choice

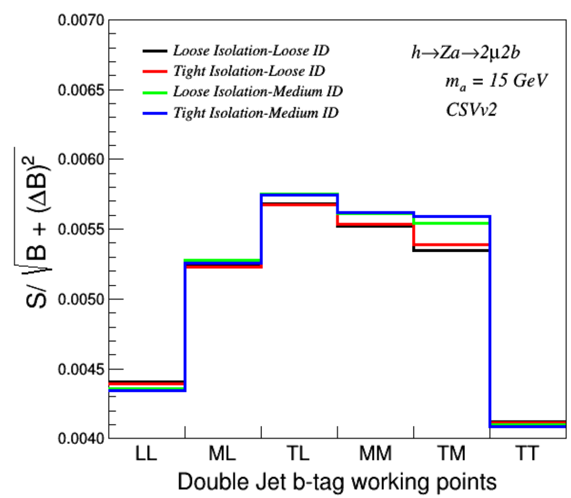

Final Selection TL is chosen

Additional Optimization

- Based on Chi Square (χ^2)
  - Exploit features and define as χ^2

$$\chi^2 = \chi^2_{b\bar{b}} + \chi^2_h$$

- For h→Za→bbμμ

$$\chi_{b\bar{b}} = \frac{(m_{b\bar{b}} - m_Z)}{\sigma_{b\bar{b}}} \qquad \chi_h = \frac{(m_{b\bar{b}\mu^-\mu^+} - m_h)}{\sigma_h}$$

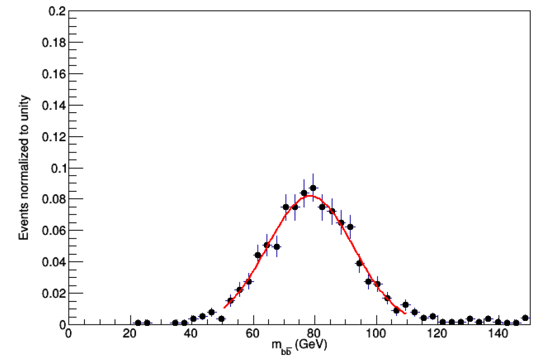

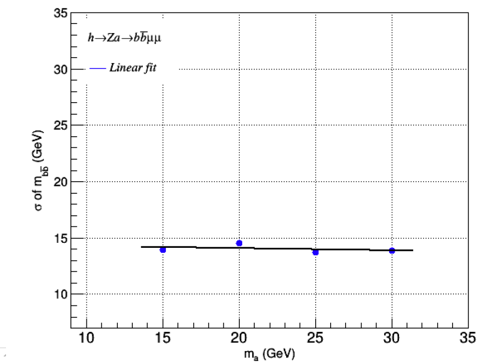

- For h→aa→bbμμ

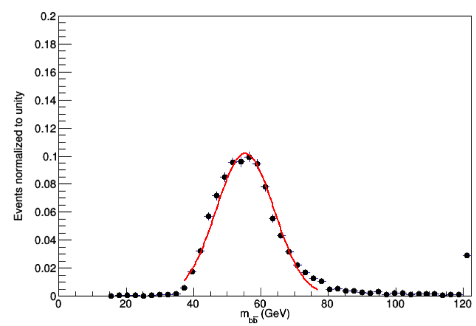

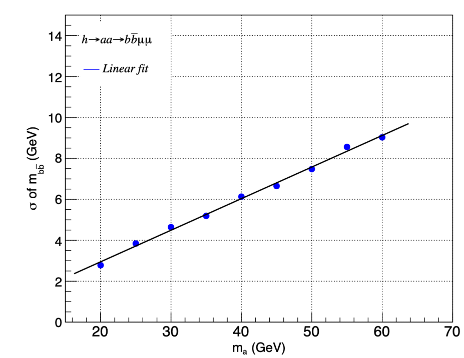

$$\chi^2 = \chi^2_{b\bar{b}} + \chi^2_h$$

$$\chi_{b\bar{b}} = \frac{(m_{b\bar{b}} - m_{\mu^-\mu^+})}{\sigma_{b\bar{b}}} \quad and \quad \chi_h = \frac{(m_{b\bar{b}\mu^-\mu^+} - m_h)}{\sigma_h}$$

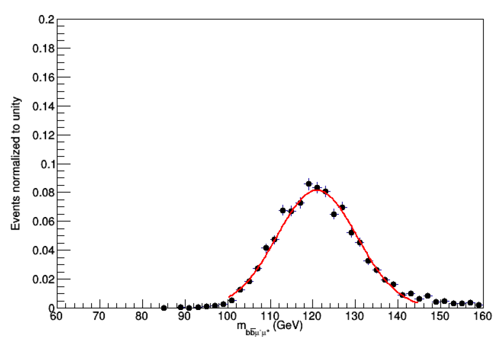

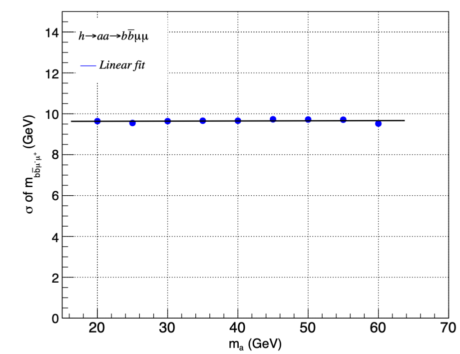

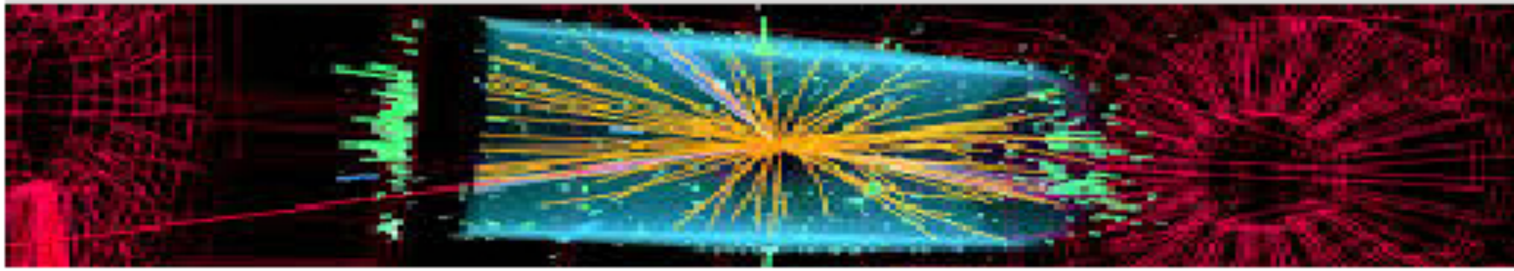

Results

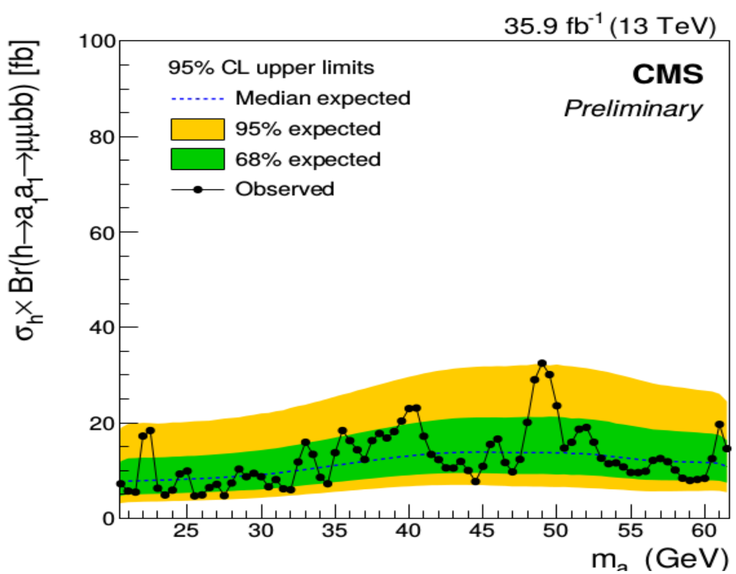

35.9 fb^{-1} (13 TeV)
CMS
Preliminary
95% CL upper limits
Median expected
95% expected
68% expected
Observed
$\sigma_h \times Br(h \to a_1 a_1 \to \mu\mu bb)$ [fb]
m_a (GeV)

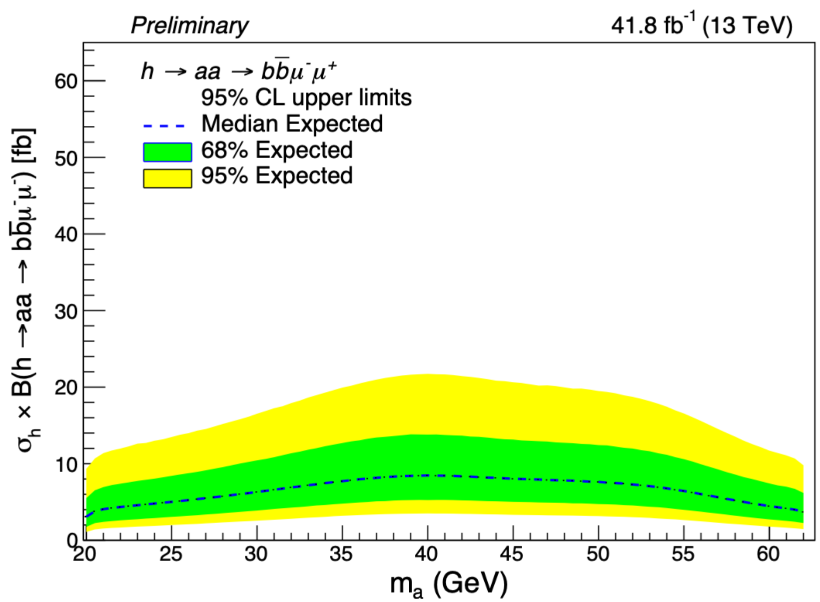

Preliminary
41.8 fb^{-1} (13 TeV)
$h \to aa \to b\bar{b}\mu^-\mu^+$
95% CL upper limits
Median Expected
68% Expected
95% Expected
$\sigma_h \times B(h \to aa \to b\bar{b}\mu^-\mu^-)$ [fb]
m_a (GeV)

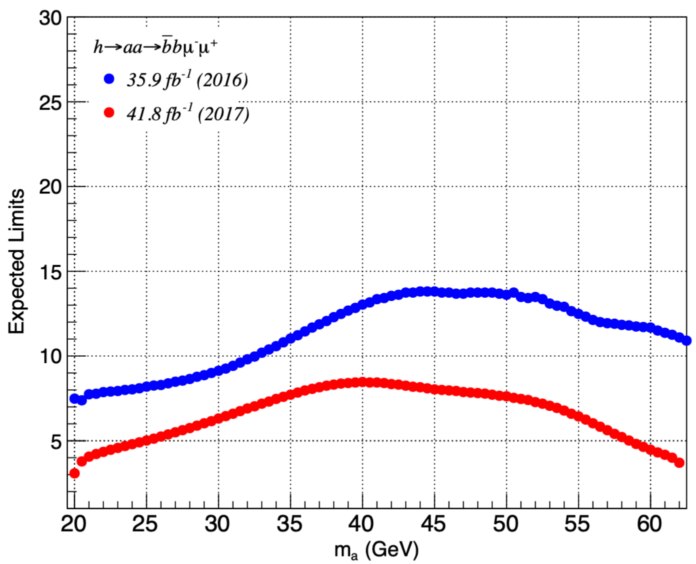

$h \to aa \to \bar{b}b\mu^-\mu^+$
35.9 fb^{-1} (2016)
41.8 fb^{-1} (2017)
Expected Limits
m_a (GeV)

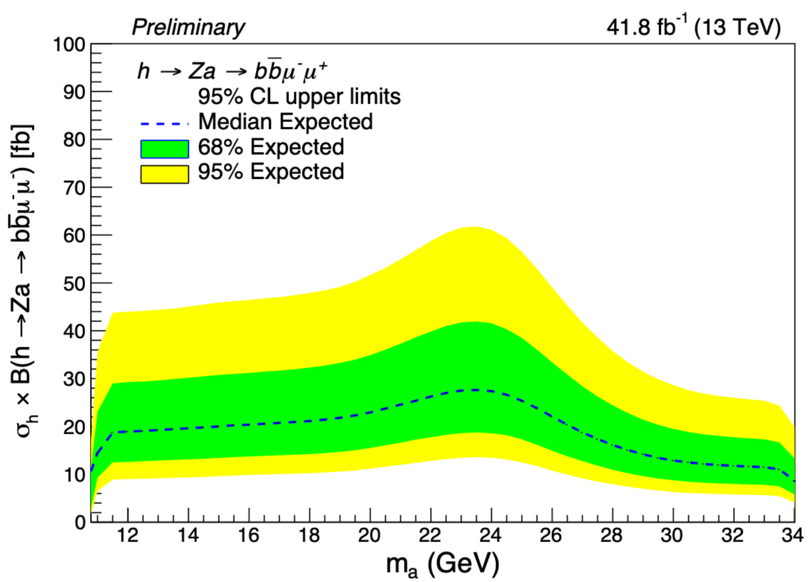

Preliminary
41.8 fb^{-1} (13 TeV)
$h \to Za \to b\bar{b}\mu^-\mu^+$
95% CL upper limits
Median Expected
68% Expected
95% Expected
$\sigma_h \times B(h \to Za \to b\bar{b}\mu^-\mu^-)$ [fb]
m_a (GeV)